Early Human Development 87 (2011) 449–453

Contents lists available at ScienceDirect

Early Human Development

journal homepage: www.elsevier.com/locate/earlhumdev

Serum chemokine levels and developmental outcome in preterm infants

Tadamune Kinjo [a,b,*], Shouichi Ohga [a,b], Masayuki Ochiai [a,b], Satoshi Honjo [a], Tamami Tanaka [c], Yasushi Takahata [c], Kenji Ihara [a,b], Toshiro Hara [a,b]

[a] Department of Pediatrics, Graduate School of Medical Sciences, Kyushu University, Fukuoka, Japan
[b] Comprehensive Maternity and Perinatal Care Center, Kyushu University Hospital, Fukuoka, Japan
[c] Department of Pediatrics, Fukuoka National Hospital, Fukuoka, Japan

ARTICLE INFO

Article history:
Received 2 July 2010
Received in revised form 10 March 2011
Accepted 17 March 2011

Keywords:
Very low birth weight infant
Chemokine
CXCL8
CCL2
Outcome

ABSTRACT

Background: Cytokines and chemokines during perinatal period may involve the neurological development of newborns.
Aims: We investigated the association of circulating chemokines during neonatal period with the outcome of premature infants.
Study design: The prospective study enrolled 29 very low birth weight (<1500 g) and appropriate-for-date infants having no underlying diseases. Serum concentrations of chemokines (CXCL8, CXCL9, CXCL10 and CCL2) and cytokines at birth and 4 weeks postnatal age were measured. Developmental quotients (DQ) at 3 years of age by the Kyoto Scale of Psychological Development were studied for the association with chemokine/cytokine levels and clinical variables including chorioamnionitis, Apgar scores, ventilator treatment and supplemental oxygen.
Results: CXCL8 levels at birth and days of ventilator treatment were negatively, CCL2 levels at 4 weeks after birth and 5-minute Apgar scores were positively correlated with the DQ of postural–motor (P–M) area at 3 years of age, respectively (CXCL8: correlation coefficient [CC] = −0.394, $p = 0.037$, ventilation: CC = −0.518, $p = 0.006$, CCL2: CC = 0.528, $p = 0.013$, and Apgar score: CC = 0.521, $p = 0.005$). Infants showing both ≥50 pg/ml of CXCL8 at birth and <250 pg/ml of CCL2 4 weeks after birth had lower DQ of P–M than those who did not ($p < 0.001$). Multivariate analyses indicated that CCL2 levels at 4 weeks of age were higher in infants who attained normal DQ of P–M (≥85) (adjusted mean, 338.4 [95% confidence interval, 225.5–507.8]) than in those who did not (<85) (159.0, [108.2–233.7]) ($p = 0.019$).
Conclusion: Circulating patterns of CXCL8 (IL-8) and CCL2 (MCP-1) during the neonatal period might affect the neurological development of preterm infants.

© 2011 Elsevier Ireland Ltd. All rights reserved.

1. Introduction

Feto-maternal responses to inflammation alter the outcomes of pregnancy ranging from the abortion to the intrauterine growth retardation and premature birth. Fetal inflammatory response syndrome (FIRS) is defined as the *in utero* cytokine storm represented by the elevation of inflammatory cytokines such as interleukin (IL)-6, IL-1β and tumor necrosis factor (TNF)-α in amniotic fluids and/or cord bloods [1]. Increased levels of these cytokines have been reported to be an independent risk factor for severe neonatal morbidity [1–4]. Not only are the direct effects of such inflammatory cytokines, but also the pro-/anti-inflammatory balance critical for the organogenesis. Inappropriate production of IL-10, anti-inflammatory cytokine, in the fetus and newborn could contribute to the postnatal evolution of chronic lung diseases [5]. Recently, increased concentrations of inflammatory cytokines in the fetal plasma have been implicated in the formation of white matter lesions and subsequent cerebral palsy (CP) [1–4]. Excessive production of cytokines in the intrathecal space accounts for the brain damages of infants with central nervous system (CNS) infection [6,7]. Several lines of clinical studies reported the association between high levels of IL-1β, IL-6 and TNF-α in the fetal and newborn circulations and the neurological outcome of preterm infants [1,4]. Delicate balance of cytokines and growth factors could affect the developing brain of premature infants over the perinatal periods. The effects of inflammatory mediators on the neurological outcomes of preterm infants have not reached a conclusion.

Chemokine primarily serves as a chemotactic factor in the trafficking of leukocytes into the sites of inflammation, by inducing the

Abbreviations: FIRS, fetal inflammatory response syndrome; IL, interleukin; TNF, tumor necrosis factor; CP, cerebral palsy; CNS, central nervous system; CC, correlation coefficient; MCP, monocyte chemoattractant protein; VLBW, very low birth weight; AGA, appropriate-for-gestational age; RDS, respiratory distress syndrome; KSPD, Kyoto Scale of Psychological Development; DQ, Developmental quotient.

* Corresponding author at: Department of Pediatrics, Comprehensive Maternity and Perinatal Care Center, Kyushu University Hospital, 3-1-1 Maidashi, Higashi-ku, Fukuoka, Japan 812-8582. Tel.: +81 92 642 5421; fax: +81 92 642 5435.
E-mail address: kinjo@pediatr.med.kyushu-u.ac.jp (T. Kinjo).

0378-3782/$ – see front matter © 2011 Elsevier Ireland Ltd. All rights reserved.
doi: 10.1016/j.earlhumdev.2011.03.008

adhesion to endothelial cells and transendothelial migration. The chemokine and its-receptor system has been implicated in the unique immune responses elicited in CNS diseases including trauma, ischemia and multiple sclerosis. Activations of CC ligand 2 (CCL2)/CC receptor 2 (CCR2), and CXCL8/CXCR2 promote macrophage and neutrophil infiltration, respectively, into the lesioned parenchyma after brain injury [8–10]. On the other hand, constitutive brain expression of chemokines and their receptors might modulate neuroprotection, neurogenesis and neurotransmission [11]. CXCL8 (IL-8) is one of the main players in FIRS [1]. CCL2 (monocyte chemoattractant protein-1: MCP-1) productions increase during pregnancy, suggesting the local modulation of immune system [12]. However, chemokines have been scarcely reported to involve the fetal and neonatal brain damages. Only two studies indicated the association of cord blood CXCL8 levels with the development of CP in preterm infants [3,4].

In the present study, we prospectively determined chemokine/cytokine levels at birth (acute phase) and 4 weeks postnatal age (stabilized phase) of preterm infants having no underlying diseases, and then assessed the development scores. Changing pattern of CXCL8 and CCL2 levels was associated with the outcome at 3 years of age. The role of chemokines in the brain development of premature infants was discussed.

2. Materials and methods

2.1. Subjects

The study subjects consisted of 29 live-born infants with <1500 g birth weight (very low birth weight, VLBW) and appropriate-for-gestational age (AGA) who were admitted to Kyushu University Hospital between January 2002 and December 2007. Sixty six of 84 VLBW and AGA survivors were followed at 3 years of age. Exclusion criteria were infants under 24 gestational weeks and having chromosomal aberrations, congenital anomalies, severe bronchopulmonary dysplasia, CNS infections, and underlying inherited diseases. To minimize the effects on cytokine and chemokine productions, infants who received steroid therapy within 4 weeks after birth were excluded. Informed consents were obtained from all parents having normal mentality. The Ethics Committee of Kyushu University approved the study.

2.2. Antenatal and neonatal clinical data

Clinical characteristics of 29 infants (male/female = 16/13) are shown in Table 1. Median gestational age and birth weight were 27.6 weeks and 1038 g, respectively. Chorioamnionitis was clinically or histologically determined [13]. Antenatal steroid use, cesarean delivery, chorioamnionitis, Apgar scores, respiratory distress syndrome (RDS), ventilator treatment and supplemental oxygen were used as clinical variables for statistical analyses. Four infants developed CP, and two of them had periventricular leukomalacia. Twenty six infants showed no abnormal brain echograms.

2.3. Measurement of serum concentrations of chemokines and cytokines

Arterial or venous peripheral blood was collected from 29 infants at birth and 23 out of them at 4 weeks postnatal age. Serum was separated from blood samples and stored at −30 °C until the analysis. Concentrations of chemokines (CXCL8, CXCL9, CXCL10 and CCL2) and cytokines (IL-1β, IL-6, IL-10, TNF-α and IL-12p70) in serum samples were determined by cytometric bead array (Becton Dickinson, San Jose, CA, USA) and flow cytometry according to manufacturer's protocol. Each detection limit was 4 pg/ml.

Table 1
Antenatal and neonatal clinical data of subjects studied.

Number	29
Male:female	16:13
Gestational age, weeks	27.6 [24.1–32.6][a]
Birth weight, g	1038 [556–1466][a]
Antenatal steroids	10 (34%)
Cesarean delivery	13 (45%)
Chorioamnionitis	10 (34%)
Apgar score at 1 min	5 [1–9][a]
at 5 min	7 [3–9][a]
Respiratory distress syndrome	16 (55%)
Ventilator treatment, days	14 [0–67][a]
Supplemental oxygen, days	28 [0–90][a]
Sepsis	3 (10%)
Patent ductus arteriosus[b]	3 (10%)

[a] Median [range].
[b] Ligation-required patients.

2.4. Developmental outcome

Developmental outcome was assessed in all infants at 3 years of age, by trained psychologists using the Kyoto Scale of Psychological Development (KSPD) that is a standardized developmental test for Japanese children [14,15]. Developmental performance on KSPD is expressed as the developmental age for three behavior areas (postural–motor [P–M], cognitive–adaptive [C–A], and language–social [L–S]) and for all areas. Developmental quotients (DQ) were calculated; the developmental age divided by the corrected age was then multiplied by 100. Developmental outcome was classed as normal for DQ of KSPD ≥ 85.

2.5. Statistical analysis

Statistical analyses were performed using STATA Statistical Software 10.0 version (Stata Corporation, College Station, TX, USA). Correlations between continuous variables were assessed with the Spearman's correlation coefficient. Chemokine/cytokine levels at birth and 4 weeks after birth were compared by Wilcoxon signed-rank test. Relations between clinical variables or chemokines and the categorized developmental outcome were examined with Wilcoxon rank-sum test. The optimal cut-off points of CXCL8 levels at birth and CCL2 levels at 4 weeks postnatal age to predict the developmental outcome were determined by the analysis of receiver operating characteristics (ROC) curve. Multiple linear regression analyses were used to examine the relations between serum levels of chemokines and developmental outcome. A p-value <0.05 was considered statistically significant.

3. Results

3.1. Clinical variables and the outcome at 3 years of age

Apgar scores both 1 and 5 min correlated positively, while the duration of ventilator treatment (days) did negatively with the DQ of all three areas (Table 2). Days of supplemental oxygen treatment correlated inversely with the DQ of P–M marginally, and L–S area. Infants with RDS had significantly lower DQ of C–A area than those without RDS ($p = 0.045$). There were positive associations between Apgar scores at 1 min and at 5 min, or ventilator treatment and supplemental oxygen (days), respectively (Apgar scores at 1 min and at 5 min: correlation coefficient [CC] = 0.871, $p < 0.001$, ventilator treatment and supplemental oxygen: CC = 0.761, $p < 0.001$). Both days of ventilator treatment and supplemental oxygen correlated negatively with Apgar scores at 5 min, respectively (ventilator treatment: CC = −0.724, $p < 0.001$, supplement oxygen: CC = −0.606, $p = 0.001$). No other variables were associated with the DQ of any areas at 3 years of age.

Table 2
Correlation between clinical variables and developmental outcome (n = 29).

	DQ at 3 years of age		
	P–M area	C–A area	L–S area
Apgar score at 1 min	0.016 (0.454)[a]	0.005 (0.530)[a]	0.022 (0.430)[a]
at 5 min	0.005 (0.521)[a]	0.008 (0.496)[a]	0.005 (0.522)[a]
Ventilator treatment (days)	0.006 (−0.518)[a]	0.001 (−0.593)[a]	0.003 (−0.546)[a]
Supplemental oxygen (days)	0.049 (−0.372)[a]	0.119 (−0.294)[a]	0.028 (−0.415)[a]

[a] p-value (correlation coefficient). Spearman's correlation coefficient.

3.2. Chemokine and cytokine levels during the neonatal period

Serum concentrations of all 4 chemokines and 3 of 5 cytokines (IL-6, IL-10, IL-12p70) at birth were significantly higher than those at 4 weeks of postnatal age (Table 3).

3.3. Chemokine and cytokine levels at birth and the outcome at 3 years of age

CXCL8 levels correlated inversely with the DQ of all area (P–M area: CC = −0.394, p = 0.037, Fig. 1a, C–A area: CC = −0.448, p = 0.017, L–S area: CC = −0.403, p = 0.032). Serum levels of IL-1β correlated negatively with the DQ of P–M and C–A area, respectively (P–M area: CC = −0.382, p = 0.043, C–A area: CC = −0.427, p = 0.023). IL-6 levels correlated negatively with the DQ of C–A area (CC = −0.465, p = 0.013). Serum levels of IL-1β and IL-6 correlated positively with CXCL8 levels, respectively (IL-1β: CC = 0.465, p = 0.013, IL-6: CC = 0.513, p = 0.006). Five out of 6 infants with <50 pg/ml of CXCL8 at birth showed normal DQ (≥85) of P–M area (Fig. 1a, open circles). No other correlations were found between the levels of chemokines (CXCL9, CXCL10 and CCL2) or cytokines (IL-10, TNF-α and IL-12p70) at birth and any area of KSPD (*data not shown*).

3.4. Chemokine levels at 4 weeks of age and the outcome at 3 years of age

As for the associations between chemokines/cytokines 4 weeks after birth and KSPD at 3 years of age, only CCL2 levels correlated positively with the DQ of P–M area (CC = 0.528, p = 0.013, Fig. 1b). Seven out of 8 infants showing ≥250 pg/ml of CCL2 had normal DQ of P–M area. The DQ scores of P–M area in infants showing ≥250 pg/ml of CCL2 at a month of age were higher than in those showing less than the level (p = 0.002). Among 15 infants with <250 pg/ml of CCL2 at 4 weeks of age, 10 out of 11 infants who had low DQ showed high CXCL8 levels at birth (≥50 pg/ml). Infants who showed both ≥50 pg/ml of CXCL8 at birth and <250 pg/ml of CCL2 at 4 weeks of age had lower DQ of P–M than those who did not (p<0.001, Fig. 2). On the other hand, among infants with ≥50 pg/ml of CXCL8 at birth, infants having normal DQ of P–M area at 3 years of age (Fig. 1, closed triangles) showed higher CCL2 levels a month after birth than infants having low DQ of P–M area at 3 years of age (p = 0.015).

Table 3
Chemokine and cytokine levels at birth and at 4 weeks postnatal age (n = 23).

	At birth	4 weeks after birth	p-value
CXCL8(pg/ml)	119.7 [<4–10,000][a]	<4 [<4–7289.1][a]	0.001[b]
CXCL9 (pg/ml)	593.0 [14.8–4685.1][a]	472.7 [81.7–1111.1][a]	0.048[b]
CXCL10 (pg/ml)	1193 [<4–10,000][a]	473.7 [111.8–1171.0][a]	0.002[b]
CCL2 (pg/ml)	609.2 [74.6–10,000][a]	199.4 [82.8–653.2][a]	0.006[b]
IL-1β (pg/ml)	<4 [<4–20,000][a]	<4 [<4–67.5][a]	0.068[b]
IL-6 (pg/ml)	13.7 [<4–20,000][a]	<4 [<4–410.2][a]	0.001[b]
IL-10 (pg/ml)	5.5 [<4–192.5][a]	<4 [<4–14.6][a]	0.003[b]
IL-12p70 (pg/ml)	<4 [<4–349.2][a]	<4 [<4–30.9][a]	0.018[b]
TNF-α (pg/ml)	<4 [<4–744.6][a]	<4 [<4–15.0][a]	0.115[b]

[a] Median [range].
[b] Wilcoxon signed-rank test.

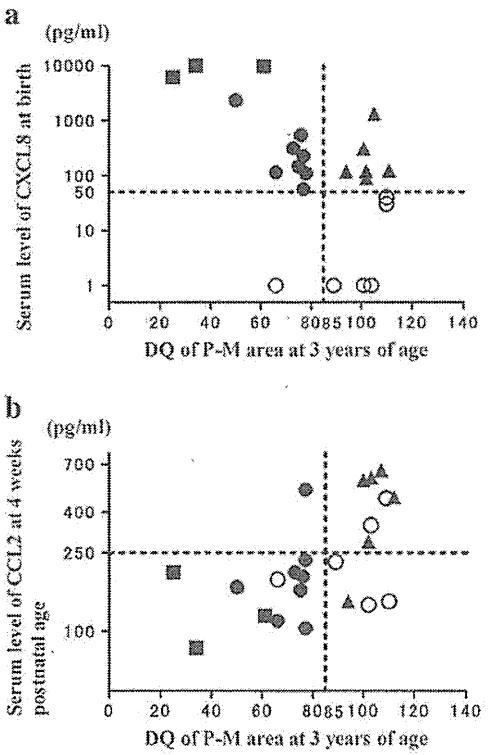

Fig. 1. Correlations with the developmental quotients (DQ) of P–M area at 3 years of age. (a) CXCL8 levels at birth (CC = −0.394, p = 0.037). Six infants having only the data at birth were omitted. (b) CCL2 levels at 4 weeks postnatal age (CC = 0.528, p = 0.013). The vertical axes are logarithmic scales. Closed squares (■) represent cerebral palsy (CP) infants. Open circles (○) represent infants who showed <50 pg/ml of CXCL8 at birth. Closed triangles (▲) represent infants who showed ≥50 pg/ml of CXCL8 at birth with normal DQ (≥85) of P–M area at 3 years of age. Five of 6 infants with <50 pg/ml of CXCL8 at birth showed normal DQ of P–M area. Among 15 infants with <250 pg/ml of CCL2 at 4 weeks of age, 10 out of 11 cases with low DQ had ≥50 pg/ml of CXCL8 at birth.

3.5. Multivariate analysis

Multiple linear regression was used to obtain adjusted means of CXCL8 levels at birth and CCL2 levels at 4 weeks postnatal age according to categorized DQ of P–M area at 3 years of age allowing for Apgar scores at 5 min and serum levels of these two chemokines. Log-transformed values of CXCL8, CCL2, Apgar score at 5 min were calculated for the skewed distributions. CCL2 levels at 4 weeks postnatal age and Apgar scores at 5 min were higher in the infants with normal DQ of P–M area than in those with low DQ even for the adjusted (Table 4).

4. Discussion

The notable finding of this study was that serum CCL2 levels at 4 weeks of age correlated positively with the 3-year-old DQ of P–M area in VLBW infants. The CCL2 levels were indicated as an independent factor for achieving normal DQ of P–M area. High CXCL8 levels at birth were associated with low DQ of P–M area at 3 years of age. The combination of high CXCL8 levels at birth and low CCL2 levels 4 weeks after birth was at risk of the low DQ. Whereas, infants showing high CXCL8 levels at birth and sustained high CCL2 levels attained normal DQ of P–M area at 3 years of age. These results

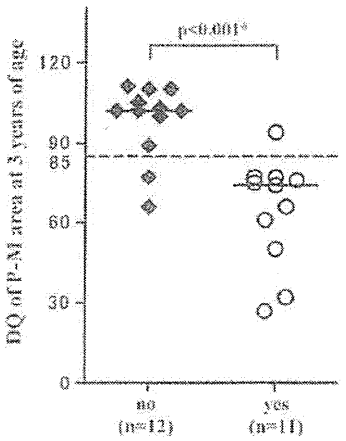

Fig. 2. The DQ scores of P–M area at 3 years of age according to the chemokine pattern. Infants who showed both ≥50 pg/ml of CXCL8 at birth and <250 pg/ml of CCL2 4 weeks after birth had lower DQ of P–M area at 3 years of age than those who did not ($p<0.001$). * Wilcoxon rank-sum test.

suggested that the chemokine balance during the first month of life might contribute to the neurological development of preterm infants.

There is limited information about the involvement of chemokines in fetal and neonatal brain damages. Huang et al. [3] first reported that cord blood levels of CXCL8 (IL-8), a mediator from monocytes, but not myeloperoxidase, another mediator from granulocytes, was correlated to CP in premature infants. They speculated that activations of both premature monocytes and granulocytes were involved in preterm delivery, but only monocyte activation was correlated with premature infants' CP. Recently, Hansen-Pupp et al. [4] reported that increased concentrations of cord blood CXCL8, low Apgar score (<7 at 5 min), and severe cerebral damage (grade III intraventricular hemorrhage and/or white matter damage) was the most predictive combination of variables for the evolution of CP. Increased concentrations of IL-1β, IL-6 and TNF-α in amniotic fluid and/or cord blood have been reported to be at risk of developing CP and/or white matter lesions [1–4]. In the current study, serum CXCL8 levels at birth correlated negatively with the DQ of all three areas. Although serum IL-1β levels at birth correlated inversely with the DQ of P–M and C–A area, and serum IL-6 levels at birth correlated inversely with the DQ of C–A area at 3 years of age, no other cytokines (TNF-α, IL-10 and IL-12p70) correlated with the neurological outcome at 3 years of age. IL-1β levels were undetectable (Table 3). This discrepancy might be explained by the difference in clinical severity of subjects. All infants in this study attained stable conditions within the first month of life, as shown in the decline of cytokine and chemokine levels. No infants had moderate to severe white matter lesions although four infants developed CP. IL-6 and CXCL8 (IL-8) are significantly produced from neonatal mononuclear cells [16,17]. In the large study using cord blood samples, CCL2, macrophage inflammatory protein (MIP)-1β and CXCL8 levels were higher than the levels of other cytokines and growth factors (IL-1β, IL-2, IL-4, IL-5, IL-6, IL-7, IL-10, IL-12p70, IL-13, IL-17, interferon-γ, TNF-α, granulocyte-colony stimulating factor and granulocyte-macrophage-colony stimulating factor). Of all inflammatory cytokines, IL-6 levels were at the highest, and were closely correlated with CXCL8 and CCL2 levels [18]. In this line, the magnitude of inflammation in the subjects might have statistical power to detect the association between chemokines and subnormal DQ. Perinatal chemokines may portend the development of VLBW infants.

Table 4
Apgar scores, ventilator treatment, CXCL8 levels at birth and CCL2 levels at 4 weeks postnatal age according to the developmental quotients (DQ) of P–M area at 3 years of age.

	The DQ of P–M area at 3 years of age		
	≥85 (n=11)	<85 (n=12)	p-value
Apgar scores at 5 min	8.0 [7.4–8.7][a]	6.1 [5.2–7.1]	0.003[c]
	7.8 [6.8–8.9][b]	6.3 [5.5–7.1][b]	0.035[d]
Ventilator treatment (days)	3.6 [1.3–10.0][a]	10.1 [5.8–17.5]	0.043[c]
	4.3 [1.7–10.7][b]	8.6 [3.6–20.6][b]	0.310[d]
CXCL8 at birth (pg/ml)	35.5 [6.7–188.2][a]	364.9 [68.9–1933.7][a]	0.033[c]
	84.5 [13.3–537.8][b]	165.0 [28.8–945.6][b]	0.641[d]
CCL2 at 4 weeks postnatal age (pg/ml)	316.1 [209.4–477.2][a]	169.3 [125.1–229.1][a]	0.027[c]
	338.4 [225.5–507.8][b]	159.0 [108.2–233.7][b]	0.019[d]

Log-transformed values of CXCL8, CCL2, Apgar scores at 5 min and days of ventilator treatment were used because of their skewed distributions. Adjusted means of CXCL8 levels at birth and CCL2 levels at 4 weeks after birth were calculated according to the categorized DQ of P–M area at 3 years of age allowing for Apgar scores at 5 min and levels of the two chemokines. Adjusted means of Apgar scores at 5 min and days of ventilator treatment were calculated allowing for levels of the two chemokines.

[a] Geometric means [95% confidence interval].
[b] Adjusted means [95% confidence interval].
[c] Wilcoxon rank-sum test.
[d] Multiple linear regression.

It was of note that high CCL2 levels at 4 weeks of age was an independent predictor of achieving normal P–M development in premature infants. There was no report on CCL2 concerning the developmental outcome of preterm infants. CCL2 (MCP-1) is one of CC chemokines, engaging in the recruitment of monocytes to the site of inflammation. It is a mediator of the neuroinflammatory processes such as neuronal degeneration occurring in CNS diseases. Astroglial and/or microglial CCL2 expressions were increased in Alzheimer's diseases, experimental autoimmune encephalomyelitis, multiple sclerosis and trauma and ischemia of the brain [8–11]. During the course of ischemia and reperfusion, various chemokines are produced in the brain including CXCL8, CCL2, CCL3, CCL4, CCL7, CX3CL1 and CXCL10 [19]. In the stroke models in rodents, both CCL2 mRNA and protein were expressed in the injured cortex [20]. CCL2-overexpressed transgenic mice showed larger infarcts and more chemoattraction of monocytes and macrophages into ischemic area than the wild-type mice [21]. By contrast, CCL2 and its receptor (CCR2) deficiency attenuated infarct volume in mice [19,22]. These changes occurred within 24 to 48 h and lasted up to 5 days. In the present study, four CP infants showed high levels of CXCL8 and CCL2 at birth (CXCL8: Fig. 1a closed squares, CCL2: 10,000 pg/ml [the highest], 7135.9 pg/ml [the second highest], 1752.5 pg/ml and 111.7 pg/ml). CCL2 levels at birth correlated positively with CXCL8 levels at birth ($CC=0.496$, $p=0.008$), as shown in the correlation between CCL2 and CXCL8 in cord blood [18]. The early CCL2 production could then be detrimental to CNS lesions in the newborn. On the other hand, CCL2 promotes the migration of newly formed neuroblasts from the neurogenic sources within the brain to the damaged areas [23]. CCL2 has a pivotal role in migration and differentiation of neural progenitor cells on hypoxia/ischemia or neuroinflammation [23–26]. CCL2 selectively upregulates astrocyte differentiation in cultured human brain-derived progenitor cells [27]. In human fetus, neural precursor cells interacted with blood-brain-barrier endothelium and differentiated in the subendothelial niche into astrocytes, neurons and oligodendrocytes under the influence of CCL2 [28]. Chemokine and its receptor system also modulate neuroprotection and neurotransmission [11]. Noradrenalin augmented CCL2 expression in astrocytes, exerting neuroprotective effects on the cytotoxic-dependent damage [29]. Constitutive expressions of CCL2 are observed in the NT2 neuronal cell lines, rat brains, and developing human brains [30–32]. In the current study, among infants with ≥50 pg/ml of CXCL8 at birth and normal DQ of P–M area (Fig. 1a closed triangles), serum CCL2 levels at 4 weeks postnatal age maintained the same levels as those at birth (*data not shown*). It may raise the possibility that sustained high levels of CCL2 within 1 month after birth had a beneficial effect on the insulted brains at birth. Dexamethasone inhibited CCL2 expression in

activated rat microglial cells [33]. Postnatal dexamethasone therapy for lung disease of prematurity may raise the risk of neuro-developmental impairment, particularly in neuromotor one [34,35]. Taken together, CCL2 production during the first month of life could have the time-dependent effects on the brain development of premature infants.

The limitations in this study were the small number of samples, and no direct analysis of cerebrospinal fluids or brain tissues. However, the present cohort recruited only appropriate-for-gestational age, VLBW infants having no underlying diseases. The management protocol was uniformed in the single tertiary center. All subjects led to a clinical relief within a month after birth. We are then convincing that the careful observation clearly disclosed the chemokine effect on the neurological outcome. CCL2 expression was necessary for the recruitment of blood-borne cells to the injury site of cerebral ischemia [36]. The localization of CCL2 in nerve terminals in the posterior pituitary suggests the direct release of the chemokine into the peripheral blood [31]. Circulating CCL2 levels might reflect the action both in and outside the CNS.

In conclusion, changing patterns of serum CXCL8 and CCL2 levels during the neonatal period might portend the development of preterm infants at 3 years of age. Later expression of CCL2 may have a neuroprotective effect on the brain damage. Further studies are needed to understand the distinct effect of chemokines on the neurological development throughout the perinatal period.

Acknowledgments

We thank Mr. Nakajima Shunji (Clinical Psychotherapist, Department of Pediatrics, Kyushu University Hospital, Fukuoka, Japan) for supporting the scoring DQ. This research was supported in part by a Grant-in-Aid for Scientific Research from Japan Society for the Promotion of Science and the Ministry of Health, Labour and Welfare of Japan.

References

[1] Gotsch F, Romero R, Kusanovic JP, Mazaki-Tovi S, Pineles BL, Erez O, et al. The fetal inflammatory response syndrome. Clin Obstet Gynecol 2007;50:652–83.
[2] Bashiri A, Burstein E, Mazor M. Cerebral palsy and fetal inflammatory response syndrome: a review. J Perinat Med 2006;34:5–12.
[3] Huang HC, Wang CL, Huang LT, Chuang H, Liu CA, Hsu TY, et al. Association of cord blood cytokines with prematurity and cerebral palsy. Early Hum Dev 2004;77: 29–36.
[4] Hansen-Pupp I, Hallin AL, Hellström-Westas L, Cilio C, Berg AC, Stjernqvist K, et al. Inflammation at birth is associated with subnormal development in very preterm infants. Pediatr Res 2008;64:183–8.
[5] Paananen R, Husa AK, Vuolteenaho R, Herva R, Kaukola T, Hallman M. Blood cytokines during the perinatal period in very preterm infants: relationship of inflammatory response and bronchopulmonary dysplasia. J Pediatr 2009;154: 39–43.
[6] Laborada G, Nesin M. Interleukin-6 and Interleukin-8 are elevated in the cerebrospinal fluid of infants exposed to chorioamnionitis. Biol Neonate 2005;88:136–44.
[7] Sherwin C, Fern R. Acute lipopolysaccharide-mediated injury in neonatal white matter glia: role of TNF-α, IL-1β, and calcium. J Immunol 2005;175:155–61.
[8] Gerard C, Rollins BJ. Chemokines and disease. Nat Immunol 2001;2(2):108–15.
[9] Savarin-Vuaillat C, Ransohoff RM. Chemokines and chemokine receptors in neurological disease: raise, retain, or reduce? Neurotherapeutics 2007;4:590–601.
[10] Schmitz T, Chew LJ. Cytokines and myelination in the central nervous system. Sci World J 2008;8:1119–47.
[11] Parsadaniantz SM, Rostène W. Chemokines and neuromodulation. J Neuroimmunol 2008;198:62–8.
[12] Briana DD, Boutsikou M, Baka S, Papadopoulos G, Gourgiotis D, Puchner KP, et al. Perinatal plasma monocyte chemotactic protein-1 concentrations in intrauterine growth restriction. Mediat Inflamm 2007;2007:65032.
[13] Shalak LF, Laptook AR, Jafri HS, Ramilo O, Perlman JM. Clinical chorioamnionitis, elevated cytokines, and brain injury in term infants. Pediatrics 2002;110:673–80.
[14] Nakai K, Suzuki K, Oka T, Murata K, Sakamoto M, Okamura K, et al. The Tohoku study of child development: A cohort study of effects of perinatal exposures to methylmercury and environmentally persistent organic pollutants on neurobehavioral development in Japanese children. Tohoku J Exp Med 2004;202:227–37.
[15] Kono Y, Mishina J, Sato N, Watanabe T, Honma Y. Developmental characteristics of very low-birthweight infants at 18 months' corrected age according to birthweight. Pediatr Int 2008;50:23–8.
[16] Angelone DF, Wessels MR, Coughlin M, Suter EE, Valentini P, Kalish LA, et al. Innate immunity of the human newborn is polarized toward a high ratio of IL-6/TNF-alpha production in vitro and in vivo. Pediatr Res 2006;60:205–9.
[17] Huang HC, Tai FY, Wang FS, Liu CA, Hsu TY, Ou CY, et al. Correlation of augmented IL-8 production to premature chronic lung disease: implication of posttranscriptional regulation. Pediatr Res 2005;58:216–21.
[18] Takahashi N, Uehara R, Kobayashi M, Yada Y, Koike Y, Kawamata R, et al. Cytokine profiles of seventeen cytokines, growth factors and chemokines in cord blood and its relation to perinatal clinical findings. Cytokine 2010;49:331–7.
[19] Dimitrijevic OB, Stamatovic SM, Keep RF, Andjelkovic AV. Absence of the chemokine receptor CCR2 protects against cerebral ischemia/reperfusion injury in mice. Stroke 2007;38:1345–53.
[20] Che X, Ye W, Panga L, Wu DC, Yang GY. Monocyte chemoattractant protein-1 expressed in neurons and astrocytes during focal ischemia in mice. Brain Res 2001;902:171–7.
[21] Chen Y, Hallenbeck JM, Ruetzler C, Bol D, Thomas K, Berman NEJ, et al. Overexpression of monocyte chemoattractant potein 1 in the brain exacerbates ischemic brain injury and is associated with recruitment of inflammatory cells. J Cereb Blood Flow Metab 2003;23:748–55.
[22] Hughes PM, Allegrini PR, Rudin M, Perry H, Mir AK, Wiessner C. Monocyte chemoattractant protein-1 deficiency is protective in a murine stroke model. J Cereb Blood Flow Metab 2002;22:308–17.
[23] Yan YP, Sailor KA, Lang BT, Park SW, Vemuganti R, Dempsey RJ. Monocyte chemoattractant protein-1 plays a critical role in neuroblast migration after focal cerebral ischemia. J Cereb Blood Flow Metab 2007;27:1213–24.
[24] Xu Q, Wang S, Jiang X, Zhao Y, Gao M, Zhang Y, et al. Hypoxia-induced astrocytes promote the migration of neural progenitor cells via vascular endothelial factor, stem cell factor, stromal-derived factor-1α and monocyte chemoattractant protein-1 upregulation in vitro. Clin Exp Pharmacol Physiol 2007;34:624–31.
[25] Liu XS, Zhang ZG, Zhang RL, Gregg SR, Wang L, Yier T, et al. Chemokine ligand 2 (CCL2) induces migration and differentiation of subventricular zone cells after stoke. J Neurosci Res 2007;85:2120–5.
[26] Belmadani A, Tran PB, Ren D, Miller RJ. Chemokines regulate the migration of neural progenitors to sites of neuroinflammation. J Neurosci 2006;26:3182–91.
[27] Lawrence DM, Seth P, Durham L, Diaz F, Boursiquot R, Ransohoff RM, et al. Astrocyte differentiation selectively upregulates CCL2/monocyte chemoattractant protein-1 in cultured human brain-derived progenitor cells. Glia 2006;53:81–91.
[28] Chintawar S, Cayrol R, Antel J, Pandolfo M, Prat A. Blood-brain-barrier promotes differentiation of human fetal neural precursor cells. Stem Cells 2009;27:838–46.
[29] Madrigal JL, Leza JC, Polak P, Kalinin S, Feinstein DL. Astrocyte-derived MCP-1 mediates neuroprotective effects of noradrenaline. J Neurosci 2009;29:263–7.
[30] Coughlan CM, McManus CM, Sharron M, Gao ZY, Murphy D, Jaffer S, et al. Expression of multiple functional chemokine receptors and monocyte chemoattractant protein-1 in human neurons. Neuroscience 2000;97:591–600.
[31] Banisadr G, Gosselin RD, Mechighel P, Kitabgi P, Rostène W, Parsadaniantz SM. Highly regionalized neuronal expression of monocyte chemoattractant protein-1 (MCP-1/CCL2) in rat brain: evidence for its colocalization with neurotransmitters and neuropeptides. J Comp Neurol 2005;489:275–92.
[32] Meng SZ, Oka A, Takashima S. Developmental expression of monocyte chemoattractant protein-1 in the human cerebellum and brainstem. Brain Dev 1999;21: 30–5.
[33] Zhou Y, Ling EA, Dheen ST. Dexamethasone suppresses monocyte chemoattractant protein-1 production via mitogen activated protein kinase phosphatase-1 dependent inhibition of Jun N-terminal kinase and p38 mitogen-activated protein kinase in activated rat microglia. J Neurochem 2007;102:667–78.
[34] Barrington K. The adverse neuro-developmental effects of postnatal steroids in the preterm infant: a systematic review of RCTs. BMC Pediatr 2001;1:1.
[35] Yeh TF, Lin YJ, Lin HC, Huang CC, Hsieh WS, Lin CH, et al. Outcomes at school age after postnatal dexamethasone therapy for lung disease of prematurity. N Engl J Med 2004;350:1304–13.
[36] Shilling M, Strecker JK, Schäbitz WR, Ringelstein EB, Kiefer R. Effects of monocyte chemoattractant protein 1 on blood-borne cell recruitment after transient focal cerebral ischemia in mice. Neuroscience 2009;161:806–12.

Interactions between residues 2228–2240 within factor VIIIa C2 domain and factor IXa Gla domain contribute to propagation of clot formation*

Tetsuhiro Soeda; Keiji Nogami; Kenichi Ogiwara; Midori Shima
Department of Pediatrics, Nara Medical University, Kashihara, Nara, Japan

Summary

Factor (F)VIII functions as a cofactor in the tenase complex responsible for phospholipid (PL)-dependent FXa generation by FIXa. We have recently reported that the FVIIIa C2 domain (residues 2228–2240) interacts with the FIXa Gla domain in this complex. We examined the role of this interaction in the generation of tenase activity during the process of clot formation, using a synthetic peptide corresponding to residues 2228–2240. The peptide 2228–2240 inhibited FVIIIa/FIXa-mediated FX activation dose-dependently in the presence of PL by >95% (IC_{50}; ~10 μM). This effect was significantly greater than that obtained by peptide 1804–1818 (IC_{50}; ~180 μM) which corresponds to another FIXa-interactive site in the light chain that provides the majority of binding energy for FIXa interaction. Peptide 2228–2240 had little effect on the prothrombin time and did not inhibit FIX activation in the coagulation process mediated by FVIIa/tissue factor or FXIa, suggesting specific inhibition of the intrinsic tenase complex. Clot waveform analysis, a plasma based-assay used to evaluate the process of intrinsic coagulation, demonstrated that peptide 2228–2240 significantly depressed both maximum coagulation velocity (|min1|) and acceleration (|min2|), reflecting the propagation of clot formation, although the clotting time was only marginally prolonged. Thromboelastography, an alternative whole blood based-assay, demonstrated that the peptide inhibited clot formation time, α-angle and maximal clot firmness, but had little effect on the clotting time. Interactions of the FVIIIa C2 domain (residues 2228–2240) with the FIXa Gla domain in the tenase complex appeared to contribute essentially to the propagation of clot formation.

Keywords

Factor VIIIa C2 domain, Factor IXa Gla domain, peptide 2228–2240, anticoagulant effect, propagation of clot formation

Correspondence to:
Keiji Nogami, MD, PhD
Department of Pediatrics, Nara Medical University
840 Shijo-cho, Kashihara, Nara 634–8522, Japan
Tel.: +81 744 29 8881, Fax.: +81 744 24 9222
E-mail: roc-noga@naramed-u.ac.jp

* An account of this work was presented at the 50th annual meeting of the American Society of Hematology, 2008, San Francisco, CA, USA. This work was supported by grants for MEXT KAKENHI 21591370.

Received: March 31, 2011
Accepted after major revision: August 1, 2011
Prepublished online: September 22, 2011
doi:10.1160/TH11-03-0203
Thromb Haemost 2011; 106: 893–900

Introduction

Factor (F)VIII, a plasma protein deficient or defective in individuals with the severe congenital bleeding disorder, haemophilia A, functions as a cofactor in the tenase complex, responsible for phospholipid (PL)-dependent conversion of FX to FXa by FIXa (1). FVIII circulates as a complex with von Willebrand factor (VWF), a macromolecule that protects and stabilises the cofactor FVIII is synthesised as a single chain molecule consisting of 2,332 amino acid residues with a molecular mass of ~300 kDa, and is arranged into three domains, A1-A2-B-A3-C1-C2, based on amino acid homology. FVIII is processed into a series of metal ion-dependent heterodimers by cleavage at the B-A3 junction, generating a heavy chain (HCh) consisting of A1 and A2 domains together with heterogeneous fragments of partially proteolysed B domain linked to a light chain (LCh) consisting of A3, C1, and C2 domains (2).

FVIII is converted into an active form, FVIIIa, by limited proteolysis by either thrombin or FXa (3). In the tenase complex, FVIIIa binds to FIXa and increases the k_{cat} for FXa formation by several orders of magnitude compared to FIXa alone (4). The A2 domain of FVIIIa interacts with the catalytic domain of FIXa, and the A3 domain interacts with the first epidermal growth factor domain (5). Although the affinity of isolated A2 for FIXa is low (K_d; ~300 nM), it amplifies the enzyme activity of FIXa by modulating an active site in the catalytic domain, and this interaction defines the cofactor activity of FVIIIa (6). Alternatively, the high affinity (K_d; ~15 nM) of the isolated FVIIIa LCh for FIXa provides the majority of the binding energy for this interaction (7). A FIXa-interactive site has been localised in the A3 domain within residues 1804–1818 (8), and we have recently identified a FIXa Gla domain-binding site within the C2 domain of FVIIIa (9). We proposed that this latter binding site was localised within residues 2228–2240, based on the inhibitory effects of a specific synthetic peptide on the activity of tenase complex and C2-FIXa interactions (9).

Naturally occurring mutations of residues 2228–2240 within C2 domain (W2229C, W2229S, Q2231H, V2232A, V2232E and

M2238V) are seen in mild/moderate haemophilia A, and have been well described in the haemophilia A database (HAMSTeRS). In addition, mutations of W2229 to C and V2232 to A are associated with development of an inhibitor (10, 11). It seems possible that these haemorrhagic phenotypes might be associated with the dysfunction of interactions between the C2 domain and FIXa. A physiological role for this relationship during intrinsic coagulation reaction remains unclear, however, and in the present study, therefore, we investigated the effects of the synthetic peptide 2228–2240 on coagulation using plasma clot waveform analysis and whole blood thromboelastography. These techniques monitor global clotting mechanisms and provide parameters that define both the initiation and the subsequent progression of clot formation. Peptide 2228–2240 significantly inhibited the later processes of clot formation to a greater extent than initiation. Interactions of residues 2228–2240 in the FVIIIa C2 domain with the FIXa Gla domain in the tenase complex seem likely to contribute to the overall propagation of coagulation.

Materials and methods

Reagents

Purified recombinant FVIII (Kogenate FS®), FVIIa (NovoSeven®) and plasma-derived human FIX (Novact M®) preparations were generous gifts from Bayer Corp. Japan (Osaka, Japan), NovoNordisk (Bagsværd, Denmark), and Chemo-Sero-Therapeutic Research Institute (Kumamoto, Japan), respectively. Human FIXa and FX (Hematologic Technologies, Inc., Essex Junction, VT, USA), FXa and FXIa (Enzyme Research Laboratories, Inc, South Bend, IN, USA), thrombin (Sigma, St Louis, MO, USA), recombinant hirudin (Calbiochem, San Diego, CA, USA), recombinant human tissue factor (TF) (Innovin®; Dade Behring, Marburg, Germany), chromogenic FXa substrate S-2222 (Chromogenix, Milano, Italy), and chromogenic FIXa substrate spectrozyme FIXa (American Diagnostica, Greenwich, CT, USA) were purchased commercially. PL vesicles containing 10% phosphatidylserine, 60% phosphatidylcholine, and 30% phosphatidylethanolamine (Sigma) were prepared using *N*-octylglucoside (12). Synthetic FVIII peptides containing residues 2228–2240 (EWLQVDFQKTMKV) and 1804–1818 (KNFVKPNETKTYFWK) and control peptide (VKMTKQFDVQLWE) comprising the 2228–2240 residues in a random sequence, were prepared by Biosynthesis (Lewisville, TX, USA). All peptides were purified by reversed-phase HPLC (purity >95%) and were confirmed by mass spectrometry analysis.

Whole blood and plasma samples

Normal human whole blood was obtained by venipuncture from four normal healthy individuals, into tubes containing a 1:9 volume of 3.8% (w/v) trisodium citrate. Normal pooled human plasma was prepared from platelet-poor plasma obtained by centrifugation of citrated whole blood from 10 normal healthy individuals for 10 minutes (min) at 1,500 g. Normal pooled plasma samples were stored at –80°C and thawed at 37°C immediately prior to use. Congenital FIX-deficient human plasma was obtained from George King (Overland Park, KS, USA).

Chromogenic assays for FXa and FIXa generation

FXa generation

Activation of FX by FIXa/FVIIIa was monitored by determining the rate of conversion of FX to FXa in a purified system (13). FIXa (1 nM) was preincubated with synthetic peptides for 2 hour (h) at 37°C. FVIII (30 nM) was activated by thrombin (10 nM) in the presence of PL (20 μM). Thrombin activity was terminated after 1 min by the addition of hirudin, and FXa generation was initiated by the addition of FX (200 nM) together with the FIXa-FVIII peptide mixture.

FIXa generation

Activation of FIX by FVIIa/TF or FXIa was monitored by assessing the rate of conversion of FIX to FIXa in a purified system. FIX (200 nM) was preincubated with synthetic peptides for 2 h at 37°C. The activation of FIX was initiated by the addition of FVIIa/TF (1 nM) or FXIa (1 nM) in the presence of PL (20 μM). Both FXa and FIXa assays were performed at 22°C in 20 mM HEPES, pH 7.2, 150 mM NaCl, 0.02% Tween20, containing 5 mM $CaCl_2$ and 0.1% bovine serum albumin. Aliquots were removed at appropriate times to assess initial rates of product formation, and added to tubes containing EDTA (100 mM final concentration) to stop the reaction. Rates of FXa or FIXa generation were determined at 405 nm using a microtiter plate reader after the addition of chromogenic substrate, S-2222 (0.46 mM final concentration) or spectrozyme FIXa (2 mM final concentration) in the presence of 33% ethylene glycol, respectively.

Prothrombin time (PT)-based assay

Normal pooled plasma (45 μl) was mixed with serial dilutions of peptide 2228–2240 (5 μl) for 2 h at 37°C. Prothrombin time (PT) was measured using standard techniques.

Clot waveform analysis

Clot waveform analysis was performed utilising the MDA-II® system (Trinity Biotech plc, Dublin, Ireland) with a modified activated partial thromboplastin time (APTT) assay and four-fold dilutions of a commercially available APTT reagent (APTT-SLA; Sysmex, Kobe, Japan) as previously described (14–16). Each

© Schattauer 2011

sample was prepared by the addition of peptide 2228–2240 (5 µl) to a) normal pooled plasma (45 µl) or to b) reconstituted normal plasma (45 µl) (FIX-deficient plasma containing 100 IU/dl FIX (corresponding to 100% FIX activity)) and incubation for 2 h at 37°C. In experiments to assess inhibition using reconstituted normal plasma, a standard curve was also prepared using FIX-deficient plasmas with serial dilutions of FIX in the absence of peptide. The four-fold dilutions of APTT-SLA (50 µl) were added to each sample, and assays commenced by adding 0.02 M $CaCl_2$ (50 µl) at 37°C. The clot waveform obtained was computer-processed using the commercial kinetic algorithm. The clotting time was defined as the time until the start of coagulation. The rate of clotting and acceleration of the clotting rate were computed respectively from the first order and second order differentials of transmittance. The minimum absolute value of the first order differential, |min 1|, represents the maximum coagulation rate, and |min 2|, the minimum absolute value of the second order differential, represents the maximum acceleration of coagulation rate.

Rotational thromboelastography (ROTEM)

ROTEM was performed using the Whole Blood Hemostasis Analyser® (Pentapharm, Munich, Germany). After venipuncture, citrated whole blood was maintained for 30 min at room temperature and was used within 3 h. Whole blood (270 µl) was preincubated with various concentrations of peptide 2228–2240 (30 µl) for 30 min at 22°C. Blood samples were recalcified with 0.2 M $CaCl_2$ (20 µl) at 37°C. Clot formation was monitored for 1 h and assessed using the standard evaluation software provided by the manufacturer. Analyses included a) the clotting time (CT; the time from the start of measurement until detection of clot firmness of 2 mm amplitude), b) clot formation time (CFT; the time from the initiation of clotting until detection of clot firmness of 20 mm amplitude), c) α-angle: the measurement of clot development kinetics, and d) maximum clot firmness (MCF; the maximum amplitude indicating the clot stabilisation).

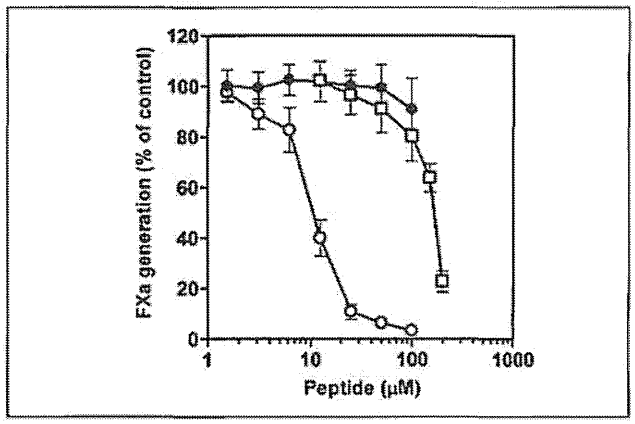

Figure 1: Effect of a C2 peptide 2228–2240 on the FVIIIa/FIXa-dependent FXa generation. Various amounts of synthetic peptides were preincubated with FIXa (1 nM) for 2 h at 37°C, and FXa generation was initiated by the addition of thrombin-activated FVIIIa (30 nM) and FX (200 nM) as described in *Methods*. The amount of FXa generated in the absence of peptide represents 100%. The percentage of FXa generated was plotted as a function of peptide concentration. The symbols used are as follows; peptide 2228–2240; ○, control random peptide; ●, peptide 1804–1818; ⌐, Experiments were performed at least three separate times, and average values and standard deviations are shown.

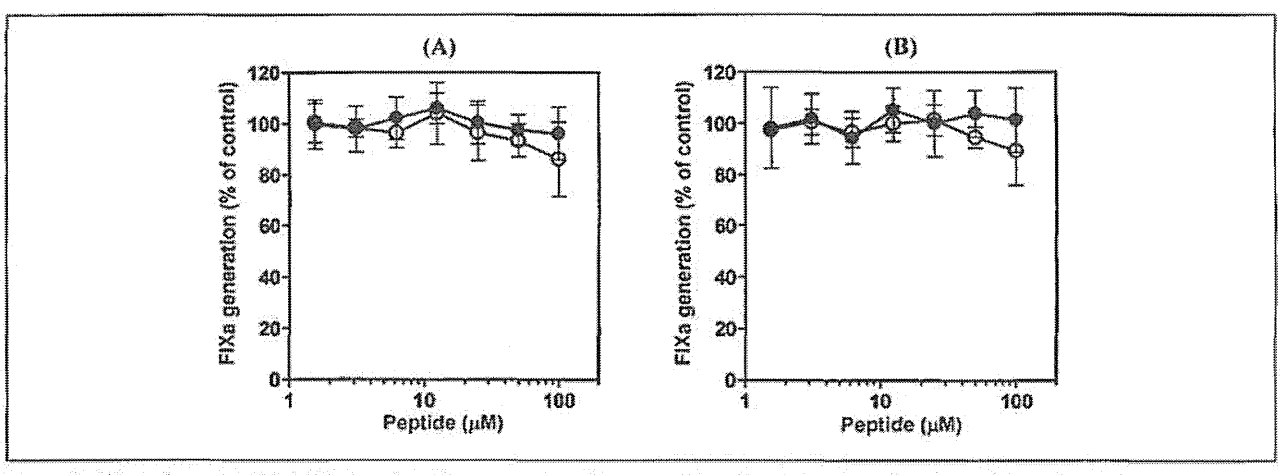

Figure 2: Effect of peptide 2228–2240 on the FIXa generation. A) Activation of FIX by FVIIa/TF: Various amounts of peptide 2228–2240 were preincubated with FIX (200 nM) for 2 h at 37°C, and FIXa generation was initiated by the addition of FVIIa/TF (1 nM) as described in *Methods*. B) Activation of FIX by FXIa: Various amounts of peptide 2228–2240 were preincubated with FIX (200 nM) for 2 h at 37°C, and FIXa generation was initiated by the addition of FXIa (1 nM) under the conditions described in *Methods*. The amount of FIXa generated in the absence of peptide represents 100%. The percentage of FIXa generated was plotted as a function of peptide concentration. The symbols used are as follows; peptide 2228–2240; ○, control peptide; ●, Experiments were performed at least three separate times, and average values and standard deviations are shown.

© Schattauer 2011

Results

Effect of peptide 2228–2240 on FIXa/FVIIIa-dependent FXa generation

Our recent study demonstrated that the peptide corresponding to FVIII residues 2228–2240 inhibited both FIXa binding to the FVIIIa C2 domain and FIXa/FVIIIa-mediated FXa generation, independently of PL (9). In the present study, we further examined the inhibitory effect of peptide 2228–2240 on tenase activity. The high affinity of the LCh of FVIIIa for FIXa contributes the majority of binding energy for FVIIIa-FIXa interaction (7), and hence, the potential of 2228–2240 was compared to the other known peptide 1804–1818, that blocks the functional interaction of FVIIIa with FIXa in FXa generation (IC_{50}; ~400 μM [8]). The peptide 2228–2240 completely inhibited the FXa generation at the maximum concentration employed, in a dose-dependent manner. The IC_{50} was ~10 μM (▶ Fig. 1). A random peptide containing the same amino acids had little effect in this assay. The inhibitory effect of peptide 2228–2240 was significantly greater than that of peptide 1804–1818 (IC_{50}; ~180 μM), although the maximum inhibitory effects of both peptides for the FXa generation were by >80%. This data suggested that the affinity of peptide 2228–2240 for FIXa might be higher than that of peptide 1804–1818. These results indicated that the 2228–2240 region in C2 as well as the 1804–1818 region in A3 contributed to the expression of tenase activity.

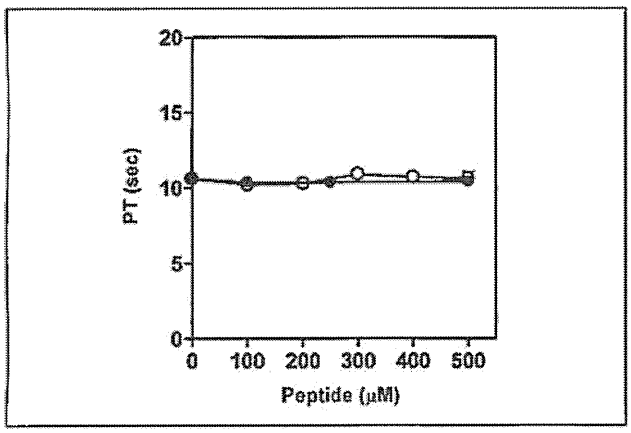

Figure 3: Effect of peptide 2228–2240 on the PT-assay using normal pooled plasma. Serial dilutions of peptide 2228–2240 were mixed with normal pooled plasma, and PT values were measured. The symbols used are as follows; peptide 2228–2240; ○, control peptide; ●, Experiments were performed at least three separate times, and average values and standard deviations are shown.

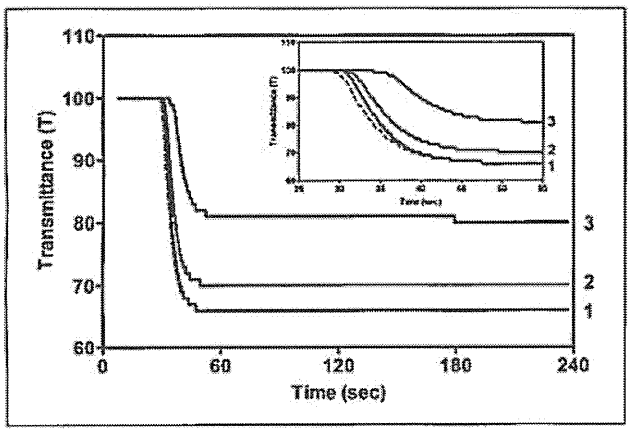

Figure 4: Effect of peptide 2228–2240 on clot waveform analysis of normal pooled plasma. Normal pooled plasma was mixed with serial dilutions of peptide 2228–2240, and the clot waveform analysis was performed. The figure illustrates representative data. The insets illustrate the time course between 25–55 seconds. The lines used are as follows, no peptide; dashed line, peptide 2228–2240 (100, 250, 500 μM, lines 1–3, respectively); solid lines.

Effect of peptide 2228–2240 on FIX activation

Peptide 2228–2240 did not affect FXa generation using Gla domainless-FIXa in place of FIXa, and we suggested, therefore, that this peptide specifically associated with the Gla domain of FIX(a) (9). Alternatively, since the Gla domain of FIX is involved in the regulation of FIX activation by both FVIIa/TF (17) and by FXIa (18), peptide 2228–2240 might have affected these reactions. We examined, therefore, the effects of this peptide on FIX activation by FVIIa/TF and FXIa in functional chromogenic assays as described in *Methods*. ▶ Figure 2A and B illustrate that peptide 2228–2240 did not appreciably inhibit the FIX activation by FVIIa/TF and by FXIa (IC_{50}; >100 μM), respectively. These results indicated that the sequence 2228–2240 was not involved in the activation of FIX.

Effect of peptide 2228–2240 on extrinsic coagulation in a PT-based assay

FV, is structurally homologous, and has a similar function to FVIII (19). Uniquely, however, FV is a cofactor in the prothrombinase complex, responsible for PL-dependent conversion of prothrombin to thrombin by FXa. The C2 domain of FV has a similar sequence to the 2228–2240 C2 region in FVIII, and we considered that peptide 2228–2240 might inhibit the activity of the prothrombinase complex (FVa/FXa/PL). We examined, therefore, the effect of this peptide on prothrombinase-dependent extrinsic coagulation in a PT-based assay. ▶ Figure 3 shows that peptide 2228–2240 had little effect on the PT at concentrations up to 500 μM, suggesting that this peptide did not affect the process of extrinsic coagulation.

© Schattauer 2011

Effects of peptide 2228–2240 on intrinsic coagulation using clot waveform analysis

The MDA® II Hemostasis system is a photo-optical automated analyser for performing clinical laboratory coagulation assays. In addition to deriving clotting times for classical APTT-based assays, it also provides the facility to simultaneously observe and quantify the changes in light transmission that occur during plasma clotting after activation and re-calcification in these routine assays. Using this system, we analysed the changes in clot dynamics mediated by the peptide 2228–2240 in tenase-dependent intrinsic coagulation. Each sample was prepared by the addition of peptide 2228–2240 to normal pooled plasma. Clot waveform analysis demonstrated that the synthetic peptide inhibited intrinsic plasma coagulation in a dose-dependent manner (▶ Fig. 4). The clotting times (representing the beginning of clot formation) and |min1| and |min2| (representing the propagation of clot formation) were significantly de-

Table 1: Effect of peptide 2228–2240 on the clot waveform analysis of normal pooled plasma.

	Clotting time (sec)	|min1| (dT/dt)	|min2| (d^2T/dt^2)
Peptide 2228–2240			
0 μM	29.8 ± 0.3	4.96 ± 0.08	0.402 ± 0.004
100 μM	30.5 ± 0.1	4.95 ± 0.13	0.406 ± 0.006
250 μM	31.5 ± 0.3	4.27 ± 0.01	0.354 ± 0.003
500 μM	35.0 ± 0.5	2.51 ± 0.03	0.199 ± 0.002
Control peptide			
500 μM	29.8 ± 0.2	4.86 ± 0.07	0.396 ± 0.001

Reactions were performed as described in *Materials and methods*. Parameter values were calculated from the data shown in Fig. 4. Experiments were performed at least three separate times, and average values and standard deviations are shown.

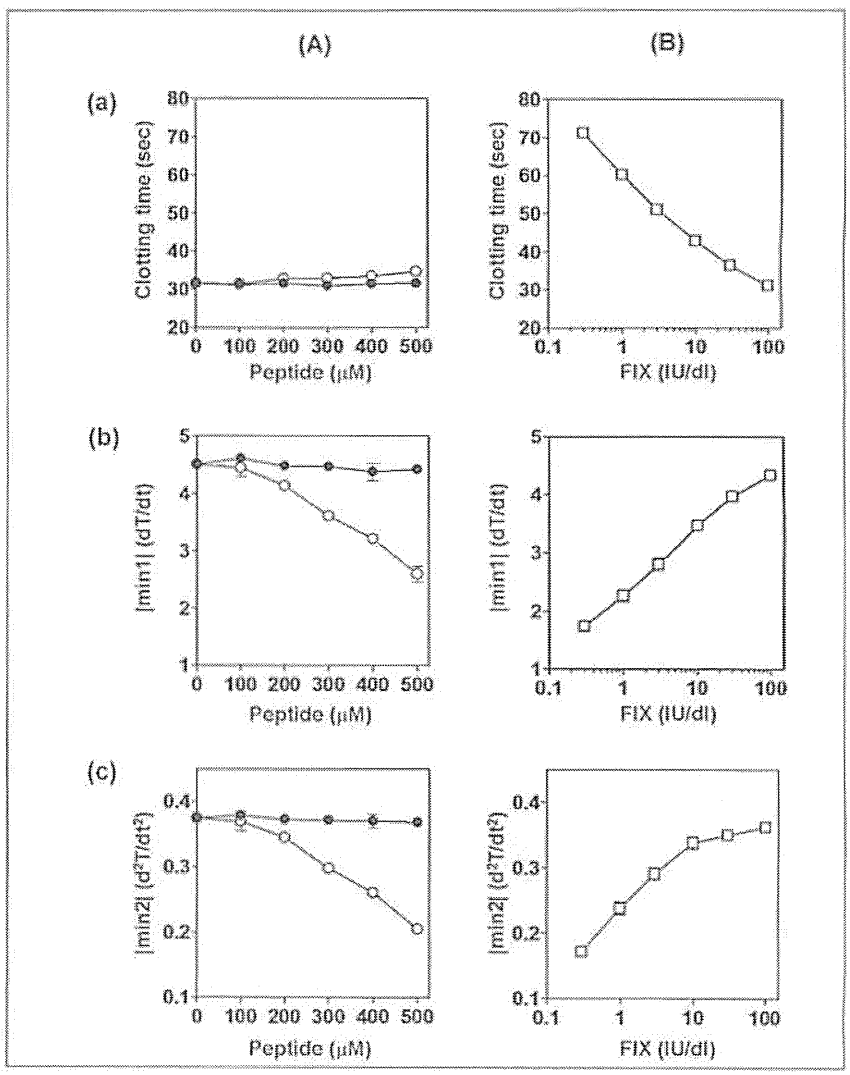

Figure 5: Effect of peptide 2228–2240 on clot waveform analysis of reconstituted normal plasma. A) Serial dilutions of peptide 2228–2240 were mixed with reconstituted normal plasma (FIX-deficient plasma with 100 IU/dl FIX). The symbols used are as follows; peptide 2228–2240; ○, control peptide; ●. B) A standard curve was prepared using FIX-deficient plasma with serial diluted FIX (0.3–100 IU/dl). Clot waveform parameters [(a) clotting time, (b) |min1| and (c) |min2|] were derived from the waveform data. Experiments were performed at least three separate times, and average values and standard deviations are shown.

© Schattauer 2011

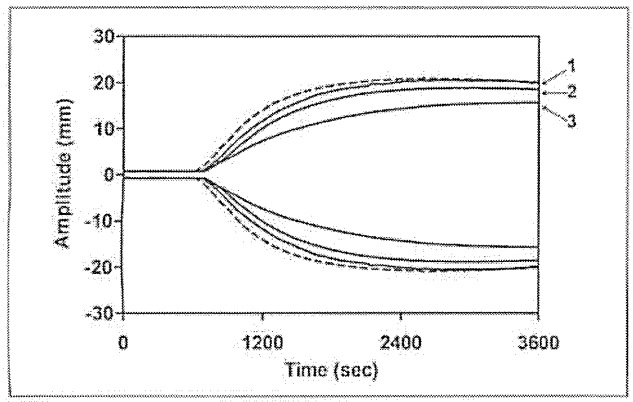

Figure 6: Effect of peptide 2228–2240 on ROTEM of normal whole blood. Whole blood was mixed with serial dilutions of peptide 2228–2240. Blood samples were recalcified with 0.2 M $CaCl_2$ at 37°C. The figure illustrates representative data. The lines used are as follows: no peptide, dashed line; peptide 2228–2240 (250, 500, 750 μM, lines 1–3, respectively), solid lines.

creased (▶ Table 1). To further examine the degree of inhibition of these parameters, we prepared samples from reconstituted normal plasma (FIX-deficient plasma containing 100 IU/dl FIX) in the presence of peptide (▶ Fig. 5A), together with standard samples of FIX-deficient plasmas containing serial dilutions of FIX in the absence of peptide (▶ Fig. 5B). The |min1| and |min2| in the presence of peptide 2228–2240 (▶ Fig. 5A) corresponded to those obtained in mixtures containing ~1 and ~2 IU/dl FIX, respectively (▶ Fig. 5B), indicating that the peptide inhibited |min1| and |min2| by ~99% and ~98%, respectively. Of interest, the effect of this peptide on the clotting time (~60% inhibition) was less than that on the |min1| and |min2|. These data suggested that peptide 2228–2240 had a significant anticoagulant effect on the process of clot formation in plasma. In contrast, peptide 1804–1818 (up to 750 μM), comprising an A3-FIXa-interactive site, did not affect any of the parameters (data not shown).

Table 2: Effect of peptide 2228–2240 on ROTEM of normal whole blood.

	CT (sec)	CFT (sec)	α-angle (°)	MCF (mm)
Peptide 2228–2240				
0 μM	649 ± 46	295 ± 64	44 ± 7	45 ± 6
250 μM	657 ± 106	376 ± 86	37 ± 7	44 ± 6
500 μM	691 ± 62	459 ± 43	31 ± 2	40 ± 3
750 μM	621 ± 71	586 ± 112	29 ± 3	37 ± 1
Control peptide				
750 μM	654 ± 131	296 ± 91	44 ± 9	44 ± 7

Reactions were performed as described in *Materials and methods*. Parameter values were calculated from the data shown in Fig. 6. Experiments were performed at least four separate times, and average values and standard deviations are shown.

Effect of peptide 2228–2240 on whole blood coagulation using ROTEM analysis

Synthetic PL vesicles are utilised in place of surface of bearing cells and platelets in APTT-based assays, and it may be that the *in vitro* conditions do not adequately reflect physiological coagulation reactions. We examined, therefore, the anticoagulant effects of peptide 2228–2240 in whole blood-based assays (ROTEM) dependent the natural surface-bound PL. ROTEM measures the shear elastic modulus during clot formation in whole blood from the beginning to propagation and subsequent fibrinolysis. We used this system to study the effect of peptide 2228–2240 on these global mechanisms. Peptide 2228–2240 inhibited the ROTEM whole blood parameters in a dose-dependent manner (▶ Fig. 6). The CFT, α-angle, and MCF were significantly decreased, whilst the CT was slightly prolonged (▶ Table 2). The findings were similar to the results obtained by clot waveform analysis, and indicated that peptide 2228–2240 depressed clot formation after the commencement of the blood coagulation reaction, consequently leading to the generation of an unstable clot.

Discussion

We have recently demonstrated that the C2 domain (residues 2228–2240) of FVIIIa contained a FIXa-interactive site (9). This site did not overlap with the PL- and VWF-interactive site(s) on the C2 domain, and a synthetic peptide corresponding to this sequence, significantly diminished tenase activity by interfering with FVIIIa-FIXa association. Interactions of the A2 domain of FVIIIa contribute to stabilisation of cofactor activity and allosteric activation of FIXa on the tenase complex, although this latter association has relatively low binding affinity (K_d; ~300 nM) (6). In contrast, the LCh of FVIIIa provides the majority of binding energy for FIXa interaction, with higher binding affinity (K_d; ~15 nM) (7). In the present study, we found that the contribution of peptide 2228–2240 to tenase activity was significantly greater than that of the already reported A3 peptide 1804–1818, with an ~18-fold lower IC_{50}. One of mechanism of the efficient down-regulation of tenase activity by peptide 2228–2240 was due to inhibition of the FVIIIa LCh-FIXa binding reaction. On the other hand, Wakabayashi et al. (20) have reported that a C2-deleted FVIII indicated not only modest reduction in the affinity for FIXa, but also reduction in stability of FVIIIa. Therefore, the reduced stability of FVIIIa allosterically might be also associated with inhibition mechanism by peptide 2228–2240.

A FIXa-interactive site comprising residues 2228–2240 in C2 domain unlikely contacts with the Gla domain simultaneously according to the model constructed by Ngo et al. (21). This discrepancy might be due to conformational change of the C2 domain. Conformational changes in C2 domain of FVIIIa upon removal of the N-terminus of the light chain (residues 1649–1689) (22) likely lead to enhance the FVIIIa affinity for PL membrane (23). This may affect the binding to Gla domain of FIXa. Furthermore, the C2

© Schattauer 2011

domain is relatively loosely docked to the remainder of FVIII molecules (21, 24), consequently the position of this domain within active-form FVIIIa on the PL surface might change easily. These can be supported by the case of residues 484–509 in A2 domain. The model proposed by Ngo showed that this region did not interact with FIXa in spite of FIXa-interactive site. Bajaj et al. (25) also demonstrated that residues 484–509 in A2 domain were not in close proximity to one face which consist of residues 558–565, 708–717, 1804–1818, and did not have contact with FIXa. Furthermore, Stoilova-McPhie et al. (26) described that it was unable to modify a FVIII-FIXa binding model including the 484–509 region. For this reason, they raised the following possibilities; the conformational change in A2 domain upon binding of the catalytic domain of FIXa, and different A2 domain arrangement between FVIII and active-form FVIIIa. Therefore, it is not so surprising that the 2228–2240 region in FVIIIa interacts with FIXa Gla domain.

Prior to evaluating interactions between the C2 domain of FVIIIa and FIXa during the process of coagulation in plasma and whole blood, we examined the specific activity of the 2228–2240 region for this interaction. The Gla domain of FIX is required for both PL binding (27) and activation of FIX by FVIIa/TF (17) and FXIa (18), and the binding site of peptide 2228–2240 was located within the Gla domain of FIX(a) (9). Hence, the effect of this peptide on reactions with other coagulation proteins associated with the Gla domain of FIX(a) was first investigated. The peptide did not interfere with PL binding (9), and furthermore did not inhibit the activation of FIX by both FVIIa/TF and FXIa in the present study. Although it is unclear at present which residues within the Gla domain of FIX are related to these activation mechanisms, the 2228–2240 peptide interactive-site(s) in the Gla domain of FIXa seem unlikely be essential for both activation. The C2 domain of FV is known to be structurally homologous to residues 2228–2240 within the FVIII molecule, and therefore, the effect of the synthetic peptide on the prothrombinase activity was also examined. The peptide did not affect the PT, however, and overall, the data suggest that peptide 2228–2240 is an inhibitor of tenase activity, specifically inhibiting the binding of FIXa to the analogous sequences in the FVIIIa C2 domain.

Physiological clot formation is widely considered to involve two reaction phases; a) an initiation phase, representing the beginning of coagulation; and b) a propagation phase, corresponding to the period between the beginning of coagulation and the growth and maturation of the clot. Conventional APTT-based assays principally measure the initiation phase of clotting, whilst clot waveform analyses and ROTEM assays directly provide parameters that reflect both reaction phases of clot formation. Peptide 2228–2240 slightly prolonged the clotting time in waveform and ROTEM assays. The clotting times were independent of the down-regulation of tenase activity mediated by peptide 2228–2240, indicating that the initial clotting stimulus was less sensitive to specific inhibition of FIXa interactions. The clot waveform parameters (|min1| and |min2|) and the ROTEM measurements (CFT, α-angle, and MCF) primarily reflect qualitative and quantitative aspects of clot development, and peptide 2228–2240 significantly inhibited these parameters. The findings indicated that these parameters were more sensitive to the specific inhibition of FVIIIa-FIXa assembly compared with the initial clotting time.

Our current results appear to be in keeping with earlier reports on the stability of recombinant FVIII variants. For example, Radtke et al. (28) reported that a disulfide bond-stabilised FVIII variant (with an A2-A3 domainal interaction), had prolonged FVIIIa activity and enhanced the ROTEM parameters CFT and α-angle but not CT. Pipe et al. (29) reported that the FVIII R531H variant with a disturbed A1-A2 domainal interactive surface, had a shortened duration of FVIIIa activity mediated by the rapid A2 dissociation from FVIIIa, and showed lower FVIII activity in two-stage clotting assay, based on chromogenic assay, compared with one-stage clotting assay which is based on the APTT principle. This discrepancy was due to the pre-incubation step of FVIII activation by thrombin in two-stage clotting assay. Wakabayashi et al. (20) have reported that a one-stage clotting assay showed the activity of the C2-deleted FVIII, which reflected defects in a variety of intermolecular interactions as well as cofactor stability, possessed approximately one-third the wild type-FVIII, whereas a thrombin generation assay revealed an ~60-fold reduction in activity of this variant compared with wild type-FVIII. It may be, therefore, that the duration of stability of FVIIIa-FIXa assembly on the tenase complex significantly contributes to the propagation of clot formation, and that conventional APTT-based assays are not sensitive to this reaction. In our current studies, the peptide 2228–2240 inhibited the formation of FVIIIa-FIXa complex, potentially leading to a significantly shortened half-life this complex.

What is known about this topic?

- Factor (F)VIIIa functions as a cofactor in the tenase complex responsible for phospholipid (PL)-dependent FXa generation by FIXa.
- We have reported that the FVIIIa C2 domain (residues 2228–2240) interacts with the FIXa Gla domain in this complex.
- This site did not overlap with the PL- and VWF-interactive site(s) on the C2 domain, and a synthetic peptide (peptide 2228–2240) corresponding to this sequence, significantly diminished tenase activity by interfering with FVIIIa-FIXa association.

What does this paper add?

- In the present study, we investigated the effects of the synthetic peptide 2228–2240 on coagulation using plasma clot waveform analysis and whole blood thromboelastography.
- The peptide 2228–2240 significantly inhibited FVIIIa/FIXa-mediated FX activation dose-dependently (IC_{50}; ~10 μM). This effect was greater than that obtained by peptide 1804–1818 (IC_{50}; ~180 μM) which corresponds to another FIXa-interactive site in the light chain.
- The peptide 2228–2240 significantly inhibited the later processes of clot formation to a greater extent than initiation.
- Interactions of residues 2228–2240 in the FVIIIa C2 domain with the FIXa Gla domain in tenase complex seem likely to contribute to the overall propagation of coagulation.

© Schattauer 2011

Under these circumstances it could be expected that peptide 2228–2240 would predominantly inhibit the parameters related to the propagation phase of clot formation.

Our present investigations also demonstrated that peptide 1804–1818 did not inhibit clot waveform parameters. The results of our FXa generation assays were highly-reproducible compared to those previously reported (8), and potential variations in the quality of the 1804–1818 peptide were not apparent. The optimum inhibitory concentration of this peptide might be higher than we utilised in our experiments (up to 750 μM), but the use of higher concentrations in plasma-based assays was restricted by non-specificity, low solubility and high viscosity. Furthermore, the only mutation within residues 1804–1818 in the A3 domain identified in the HAMSTeRS database is the substitution of W1817 to a stop codon. Although the effects mediated by peptides might assume an ensemble of conformations of which a limited set might mimic the fold in the native protein, the physiological role of these residues in the activity of the tenase complex during the intrinsic coagulation remains to be fully defined.

In conclusion, our findings have provided strong evidence that interactions between the FVIIIa C2 domain (residues 2228–2240) and the FIXa Gla domain in the tenase complex contributes to physiological clot propagation.

Acknowledgements

We thank Dr. J. C. Giddings for helpful suggestions.

Conflict of interest

T. Soeda is an employee of Chugai Pharmaceutical Co. LTD, Japan. None of the other authors declare any conflict of interest.

References

1. Mann KG, Nesheim ME, Church WR, et al. Surface-dependent reactions of the vitamin K-dependent enzyme complexes. Blood 1990; 76: 1–16.
2. Wood WI, Capon DJ, Simonsen CC, et al. Expression of active human factor VIII from recombinant DNA clones. Nature 1984; 312: 330–337.
3. Eaton D, Rodriguez H, Vehar GA. Proteolytic processing of human factor VIII. Correlation of specific cleavages by thrombin, factor Xa, and activated protein C with activation and inactivation of factor VIII coagulant activity. Biochemistry 1986; 25: 505–512.
4. van Dieijen G, Tans G, Rosing J, et al. The role of phospholipid and factor VIIIa in the activation of bovine factor X. J Biol Chem 1981; 256: 3433–3442.
5. Schmidt AE, Bajaj SP. Structure-function relationships in factor IX and factor IXa. Trends Cardiovasc Med 2003; 13: 39–45.
6. Fay PJ, Koshibu K. The A2 subunit of factor VIIIa modulates the active site of factor IXa. J Biol Chem 1998; 273: 19049–19054.
7. Lenting PJ, Donath MJ, van Mourik JA, et al. Identification of a binding site for blood coagulation factor IXa on the light chain of human factor VIII. J Biol Chem 1994; 269: 7150–7155.
8. Lenting PJ, van de Loo JW, Donath MJ, et al. The sequence Glu1811-Lys1818 of human blood coagulation factor VIII comprises a binding site for activated factor IX. J Biol Chem 1996; 271: 1935–1940.
9. Soeda T, Nogami K, Nishiya K, et al. The factor VIIIa C2 domain (residues 2228–2240) interacts with the factor IXa Gla domain in the factor xase complex. J Biol Chem 2009; 284: 3379–3388.
10. Healey JF, Barrow RT, Tamim HM, et al. Residues Glu2181-Val2243 contain a major determinant of the inhibitory epitope in the C2 domain of human factor VIII. Blood 1998; 92: 3701–3709.
11. Elder B, Lakich D, Gitschier J. Sequence of the murine factor VIII cDNA. Genomics 1993; 16: 374–379.
12. Mimms LT, Zampighi G, Nozaki Y, et al. Phospholipid vesicle formation and transmembrane protein incorporation using octyl glucoside. Biochemistry 1981; 20: 833–840.
13. Nogami K, Freas J, Manithody C, et al. Mechanisms of interactions of factor X and factor Xa with the acidic region in the factor VIII A1 domain. J Biol Chem 2004; 279: 33104–33113.
14. Matsumoto T, Shima M, Takeyama M, et al. The measurement of low levels of factor VIII or factor IX in hemophilia A and hemophilia B plasma by clot waveform analysis and thrombin generation assay. J Thromb Haemost 2006; 4: 377–384.
15. Shima M. Understanding the hemostatic effects of recombinant factor VIIa by clot wave form analysis. Semin Hematol 2004; 41 (1 Suppl 1): 125–131.
16. Shima M, Matsumoto T, Fukuda K, et al. The utility of activated partial thromboplastin time (aPTT) clot waveform analysis in the investigation of hemophilia A patients with very low levels of factor VIII activity (FVIII:C). Thromb Haemost 2002; 87: 436–441.
17. Ndonwi M, Broze GJ, Jr., Agah S, et al. Substitution of the Gla domain in factor X with that of protein C impairs its interaction with factor VIIa/tissue factor: lack of comparable effect by similar substitution in factor IX. J Biol Chem 2007; 282: 15632–15644.
18. Aktimur A, Gabriel MA, Gailani D, et al. The factor IX gamma-carboxyglutamic acid (Gla) domain is involved in interactions between factor IX and factor XIa. J Biol Chem 2003; 278: 7981–7987.
19. Church WR, Jernigan RL, Toole J, et al. Coagulation factors V and VIII and ceruloplasmin constitute a family of structurally related proteins. Proc Natl Acad Sci USA 1984; 81: 6934–6937.
20. Wakabayashi H, Griffiths AE, Fay PJ. Factor VIII lacking the C2 domain retains cofactor activity in vitro. J Biol Chem 2010; 285: 25176–25184.
21. Ngo JC, Huang M, Roth DA, et al. Crystal structure of human factor VIII: implications for the formation of the factor IXa-factor VIIIa complex. Structure 2008; 16: 597–606.
22. Saenko EL, Scandella D, Yakhyaev AV, et al. Activation of factor VIII by thrombin increases its affinity for binding to synthetic phospholipid membranes and activated platelets. J Biol Chem 1998; 273: 27918–27926.
23. Saenko EL, Scandella D. The acidic region of the factor VIII light chain and the C2 domain together form the high affinity binding site for von willebrand factor. J Biol Chem 1997; 272: 18007–18014.
24. Shen BW, Spiegel PC, Chang CH, et al. The tertiary structure and domain organization of coagulation factor VIII. Blood 2008; 111: 1240–1247.
25. Bajaj SP, Schmidt AE, Mathur A, et al. Factor IXa:factor VIIIa interaction. helix 330–338 of factor ixa interacts with residues 558–565 and spatially adjacent regions of the a2 subunit of factor VIIIa. J Biol Chem 2001; 276: 16302–16309.
26. Stoilova-McPhie S, Villoutreix BO, Mertens K, et al. 3-Dimensional structure of membrane-bound coagulation factor VIII: modeling of the factor VIII heterodimer within a 3-dimensional density map derived by electron crystallography. Blood 2002; 99: 1215–1223.
27. Freedman SJ, Blostein MD, Baleja JD, et al. Identification of the phospholipid binding site in the vitamin K-dependent blood coagulation protein factor IX. J Biol Chem 1996; 271: 16227–16236.
28. Radtke KP, Griffin JH, Riceberg J, et al. Disulfide bond-stabilized factor VIII has prolonged factor VIIIa activity and improved potency in whole blood clotting assays. J Thromb Haemost 2007; 5: 102–108.
29. Pipe SW, Saenko EL, Eickhorst AN, et al. Hemophilia A mutations associated with 1-stage/2-stage activity discrepancy disrupt protein-protein interactions within the triplicated A domains of thrombin-activated factor VIIIa. Blood 2001; 97: 685–691.

© Schattauer 2011

THE JOURNAL OF
Obstetrics and Gynaecology Research

doi:10.1111/j.1447-0756.2011.01669.x J. Obstet. Gynaecol. Res. 2011

Cervical length predicts placental adherence and massive hemorrhage in placenta previa

Kotaro Fukushima, Arisa Fujiwara, Ai Anami, Yasuyuki Fujita, Yasuo Yumoto, Atsuhiko Sakai, Seiichi Morokuma and Norio Wake

Department of Obstetrics and Gynecology, Kyushu University Hospital, Kyushu University, Fukuoka, Japan

Abstract

Aim: To evaluate the relationship between cervical length (CL) and obstetrical outcome in women with placenta previa.

Material and Methods: Eighty uncomplicated, singleton pregnancies with an antenatally diagnosed previa were categorized based on CL of over 30 mm ($n = 60$) or 30 mm or less ($n = 20$). A retrospective chart review was then performed for these cases to investigate the relationship between CL and maternal adverse outcomes.

Results: The mean CL was 38.5 ± 5.4 mm and 26.9 ± 3.2 mm and the mean gestational age at measurement was 29.2 ± 2.7 and 28.5 ± 2.7 weeks of gestation for the longer and shorter CL groups, respectively. The median estimated blood loss at cesarean section (CS) was significantly higher in the shorter CL group (1302 mL vs 2139 mL, $P = 0.023$) as was the percentage of patients with massive intraoperative hemorrhage (60.0 vs 18.3%, $P = 0.001$). In the shorter versus longer CL patients, emergent CS before 37 weeks (23.3 vs 50.0%, $P = 0.046$) and the percentage of patients with placental adherence (6.7 vs 35.0%, $P = 0.004$) were both significantly more frequent in the shorter CL group. The shorter CL was a risk factor both for massive estimated blood loss (≥2000 mL) (odds ratio 6.34, 95% confidence interval 1.91–21.02, $P \leq 0.01$) and placental adherence (odds ratio 6.26, 95% confidence interval 1.23–31.87, $P \leq 0.05$) in the multivariate analysis.

Conclusion: CL should be included in the assessment of a placenta previa given its relationship to emergent CS, cesarean hysterectomy, intraoperative blood loss and placental adherence.

Key words: cervical length, cesarean section, massive bleeding, placental adherence.

Introduction

Placenta previa complicates only 0.5% of pregnancies;[1] however, it is one of the leading causes of maternal morbidity and mortality due to antepartum and intrapartum hemorrhage. Hemorrhage typically occurs in the third trimester as the lower uterine segment becomes more defined and the internal os dilates. These changes result in tearing of the placental vessels,[2,3] which often cannot be controlled by contraction of the relatively underdeveloped myometrial layer. This can lead to massive and unpredictable hemorrhage and an emergent preterm delivery.

It is now widely accepted that an association exists between decreased cervical length (CL) and preterm labor, with a CL of less than 30 mm being associated with a relative risk for preterm birth of 3.8.[4–6] A few studies have also reported an association between decreased CL and antepartum or post-partum hemorrhage requiring delivery by emergency cesarean section (CS).[7–9] However its clinical significance is still controversial.

Received: January 24 2011.
Accepted: April 7 2011.
Reprint request to: Dr Kotaro Fukushima, Department of Obstetrics and Gynecology, Kyushu University Hospital, Kyushu University, Maidashi 3-1-1, Higashi-ku, Fukuoka 812-8582, Japan. Email: kfuku@gynob.med.kyushu-u.ac.jp
Conflict of Interest statement: None.

© 2011 The Authors
Journal of Obstetrics and Gynaecology Research © 2011 Japan Society of Obstetrics and Gynecology

Here we report the findings of a retrospective chart review of pregnancies complicated by placenta previa in which we evaluate the relationship between CL and maternal adverse outcome.

Methods

The patients included in the study were followed at or referred to the Comprehensive Maternity and Perinatal Care Unit and Department of Obstetrics and Gynecology, Kyushu University Hospital, between January 2006 and June 2010. All patients were Japanese women. The gestational age (GA) was confirmed by multiple sonographic fetal measurements during the first trimester. The study was approved by Kyushu University Hospital Ethical Review Board. The subjects were all diagnosed with placenta previa by transvaginal sonography before 34 weeks of gestation (106 cases). We excluded any patients with threatened preterm labor at the time of CL measurement. Multiple gestation, ruptured membranes, evidence of polyhydramnios, fetal growth restriction, fetal anomalies or medical disorders complicating the pregnancy were also excluded. Ultimately, 80 cases were included in the review.

CL was transvaginally measured by the following technique between 24 weeks and 33 weeks of gestation. After bladder evacuation, a sagittal plane was obtained to visualize the full length of the cervical canal. CL was then measured three times and the shortest measurement was recorded.

A CS was scheduled for approximately 37 weeks of gestation following sonographic diagnosis of a complete placental previa. If vaginal bleeding occurred prior to the scheduled CS, the patient was admitted to the hospital and delivery was decided in accordance with her clinical condition. If indicated, betamethasone i.m. and tocolytic agents were administered for the induction of fetal lung maturity. In cases of significant, ongoing active bleeding, an emergency CS was performed regardless of gestational age.

The patients were divided into two groups based on a CL longer than 30 mm (longer CL) or 30 mm or less (shorter CL). A retrospective chart review was then performed to record maternal demographic characteristics (age, gravidity, parity, prior CS, prior dilatation and curettage, history of smoking); ultrasonographic findings (CL, GA at measurement, interval to delivery, antepartum hemorrhage [APH] before measurement, placental location, type of placenta previa); and maternal outcome (GA at delivery, number of preterm labor, usage of tocolytic agents, history of APH, the number of cases resulting in an emergent CS, estimated blood loss [EBL] during CS [including amniotic fluid], the number of the cases with an EBL over 2000 mL, and the number of cases with abnormal placental adherence). The diagnosis of placental adherence included two categories, one in which the pathologic diagnosis of accreta was established following cesarean hysterectomy and the other in which the placenta was left *in situ* following attempted extraction. The latter was permitted following preoperative counseling in hemodynamically stable patients desiring conservation.

Multivariate analysis and a receiver–operator characteristics curve for CL in the prediction of massive bleeding or placental adherence were calculated using EXCELL Tokei 2010, in Japanese (Shakai Joho Service, Tokyo, Japan). Statistical analysis was performed using the Mann–Whitney test, chi-squared test, and the unpaired *t*-test programmed in GraphPad Prism (GraphPad Software, Inc., La Jolla, CA, USA). A *P*-value of less than 0.05 was considered significant.

Results

Clinical profile

Eighty patients fulfilled the inclusion criteria out of 106 pregnancies with placenta previa referred to our center and diagnosed before 34 weeks of gestation. The clinical profile of each of the studied women is listed in Table 1. The median age of the longer CL (longer than 30 mm) group and the shorter CL (30 mm or less) group was 34 (range 23–43) and 32 (range 25–40), respectively. The median gravidity and parity in the longer and shorter groups were 1 (range 0–6) and 0 (range 0–4), and 1 (range 0–4) and 0 (range 0–4), respectively. The numbers of patients with history of prior CS in the longer and shorter groups were 8 (13.3%) and 4 (20%), respectively. The numbers of patients with history of prior dilatation and curettage in the longer and shorter groups were 15 (25.0%) and 5 (25.0%), respectively. There were no significant differences between the groups.

Ultrasonographic findings

Table 2 summarizes the ultrasonographic findings. The mean CL in the longer and shorter groups was 38.5 ± 5.4 and 26.9 ± 3.2 mm, respectively. The mean GA at measurement was 29.2 ± 2.7 and 28.5 ± 2.7 weeks of gestation, respectively. The numbers of patients who had a history of unprovoked vaginal

© 2011 The Authors
Journal of Obstetrics and Gynaecology Research © 2011 Japan Society of Obstetrics and Gynecology

Table 1 Clinical profiles

Demographic profile	Longer cervix ($n = 60$)	Shorter cervix ($n = 20$)	*P*-value
Age	34 (23–43)	32 (25–40)	0.11
Gravidity	1 (0–6)	1 (0–8)	0.32
Parity	0 (0–4)	0 (0–4)	0.76
Prior CS (median [range])	0 (0–2)	0 (0–3)	0.37
Prior CS (ratio)	8 (13.3%)	4 (20.0%)	0.48
Prior DC (median [range])	0 (0–4)	0 (0–5)	0.68
Prior DC (ratio)	15 (25.0%)	5 (25.0%)	>0.99
Smoker	8 (13.3%)	1 (5.0%)	0.44

Data are presented as median (range) or as a percentage of the total number of cases (ratio). CS, cesarean section; DC, dilatation and curettage.

Table 2 Ultrasonographic findings

Ultrasonographic findings	Longer cervix ($n = 60$)	Shorter cervix ($n = 20$)	*P*-value
CL (mm)	38.5 ± 5.4	26.9 ± 3.2	**<0.001**
GA at measurement (weeks)	29.2 ± 2.7	28.5 ± 2.2	0.32
CL measurement to delivery interval (weeks)	6.6 (1.4–8.9)	4.1 (1.4–5.9)	**<0.001**
History of APH before CL measurements	5 (8.3%)	8 (40.0%)	0.29
Placental location (anterior)	2 (3.3%)	3 (15.0%)	0.10
Complete	36 (60.0%)	16 (80.0%)	0.18

Data are presented as the mean ± standard deviation, median (range) or as a percentage of the total number of cases (ratio). Values in bold are statistically significant. APH, antepartum hemorrhage; CL, cervical length; GA, gestational age.

Table 3 Maternal outcome

Maternal outcome	Longer cervix ($n = 60$)	Shorter cervix ($n = 20$)	*P*-value
GA at delivery	37.1 (28.4–38.1)	36.7 (28.7–37.7)	**<0.05**
PTL before 34 weeks	2 (3.3%)	3 (15.0%)	0.10
Tocolytic agents	15 (25.0%)	8 (40.0%)	0.26
Antepartum hemorrhage	22 (36.7%)	11 (55.0%)	0.19
GW at initial bleeding	32.0 (18.0–37.0)	26.5 (20.0–36.0)	0.11
Emergent CS (<37 W)	14 (23.3%)	10 (50.0%)	**<0.05**
Bleeding at CS (mL)	1302 (270–3576)	2139 (573–8000)	**<0.05**
Massive hemorrhage (>2000 mL including AF)	11 (18.3%)	12 (60.0%)	**<0.01**
Placental adherence	4 (6.7%)	7 (35.0%)	**<0.01**
Cesarean hysterectomy	0 (0.0%)	3 (15.0%)	**<0.05**
Retained placenta	4 (6.7%)	4 (20.0%)	0.102

Data are presented as the mean ± SD, median (range) or as a percentage of the total number of cases (ratio). Values in bold are statistically significant. AF; amniotic fluid; CS, cesarean section; GA, gestational age; GW, gestational weeks; PTL, preterm labor.

bleeding, anterior previa, and complete previa are shown in Table 2. There were no other significant differences between the groups with the exception of the interval between CL measurement and delivery ($P < 0.001$).

Maternal outcome

Table 3 summarizes maternal outcomes. The median gestational week at delivery was 37.1 (range 28.4–38.1) and 36.7 (range 28.7–37.7), the number of patients

© 2011 The Authors
Journal of Obstetrics and Gynaecology Research © 2011 Japan Society of Obstetrics and Gynecology

Table 4 Perinatal outcome

Perinatal outcome	Longer cervix ($n = 60$)	Shorter cervix ($n = 20$)	P-value
Birthweight	2662 (1302–3730)	2560 (1188–3675)	0.106
Apgar (1 min)	8 (1–9)	8 (1–9)	0.061
Apgar (5 min)	9 (4–10)	9 (4–10)	0.056
Umbilical pH	7.32 (7.01–7.41)	7.32 (6.89–7.41)	0.836

Data are presented as medians (range).

entering labor before 34 weeks was two (3.3%), and three (15.0%), and the number of patients given tocolytic agents was 15 (25.0%) and eight (40.0%) for the longer and shorter groups, respectively. The number of patients with unprovoked vaginal bleeding, the GA at initial bleeding, and the number of patients who underwent emergent CS in both groups are shown in Table 3. There were significant differences between the groups with respect to gestational weeks at delivery ($P = 0.02$), and emergent CS before 37 weeks of gestation ($P \leq 0.05$).

The median EBL at CS and the number of patients who had an EBL over 2000 mL were 1302 (range 270–3576) and 11 (18.3%), and 2139 (range 573–8000) and 12 (60.0%), for the longer and shorter groups, respectively, representing significant differences (EBL $P < 0.05$; number of patients EBL > 2000 mL $P \leq 0.01$)

The number of cases with placental adherence were four (6.7%) and seven (35.0%), for histologically confirmed accreta and electively retained placentas, respectively ($P \leq 0.01$).

The odds ratios for an emergent CS before 37 weeks, massive hemorrhage, and placental adherence in women with a shorter CL were 3.29 (95% confidential interval [CI] 1.13–29.62), 6.68 (95% CI 2.201–20.24), and 7.54 (95% CI 1.92–29.623), respectively.

Perinatal outcome

Perinatal outcomes are shown in Table 4. The median birthweight, Apgar scores at 1 min and 5 min and cord blood pH were 2662 g (range 1302–3730), 8 (range 1–9), 9 (4–10), 7.32 (7.01–7.41), and 2560 g (range 1188–3675), 8 (range 1–9), 9 (4–10), 7.32 (6.89–7.41), respectively. None of these differences was statistically significant.

Multivariate analysis

Since the number of patients with a prior cesarean, anterior placenta, and complete previa were all higher in the short cervix group, although there was no statistical significance, we then performed a multivariate analysis using these variables and CL to massive EBL (more than 2000 mL). As shown in Table 5, the odds ratio (95% CI) for history of prior CS, complete previa, anterior location and shorter cervix were 4.51 (1.03–19.73), $P \leq 0.05$; 1.99 (0.63–6.33), $P = 0.24$; 1.76 (0.42–7.41), $P = 0.04$; and 6.34 (1.23–31.87), $P \leq 0.01$), respectively (Table 5, upper panel). A multivariate analysis using these four variables for placental adherence is shown in Table 5, lower panel. The odds ratio (95% CI) for history of prior CS, complete previa, anterior location and shorter cervix were 2.58 (0.35–19.26), $P = 0.36$; 2.38 (0.37–15.12), $P = 0.36$; 10.96 (2.09–57.45), $P \leq 0.01$; and 6.26 (1.23–31.87), $P \leq 0.05$), respectively (Table 5, lower panel).

Table 5 Multivariate analysis for massive estimated blood loss (EBL) (≥2000 mL) or placental adherence

	Odds ratio	95% Confidence interval	P-value
Massive EBL (>2000 mL)			
History of prior CS	4.51	1.03–19.73	**<0.05**
Complete	1.99	0.63–6.33	0.24
Anterior location	1.76	0.42–7.41	0.44
Shorter CL (30 mm or less)	6.34	1.91–21.02	**<0.01**
Placental adherence			
History of prior CS	2.58	0.35–19.26	0.36
Complete	2.38	0.37–15.12	0.36
Anterior location	10.96	2.09–57.54	**<0.01**
Shorter CL (30 mm or less)	6.26	1.23–31.87	**<0.05**

Values in bold are statistically significant. CL, cervical length; CS, cesarean section.

Predictive values

Based on the receiver operating characteristic curve at a cut-off point 30 mm for CL, the sensitivity, specificity, positive predictive value (PPV) and negative predictive value were 63.6, 81.2, 20.6, and 96.7%, respectively, for predicting cases at high risk for placental adherence with area under the curve of 0.680. The sensitivity, specificity, PPV and negative predictive value were 52.2, 86.0, 14.0, and 89.7%, respectively, for the prediction of massive hemorrhage with an area under the curve of 0.592 (Fig. 1).

© 2011 The Authors
Journal of Obstetrics and Gynaecology Research © 2011 Japan Society of Obstetrics and Gynecology

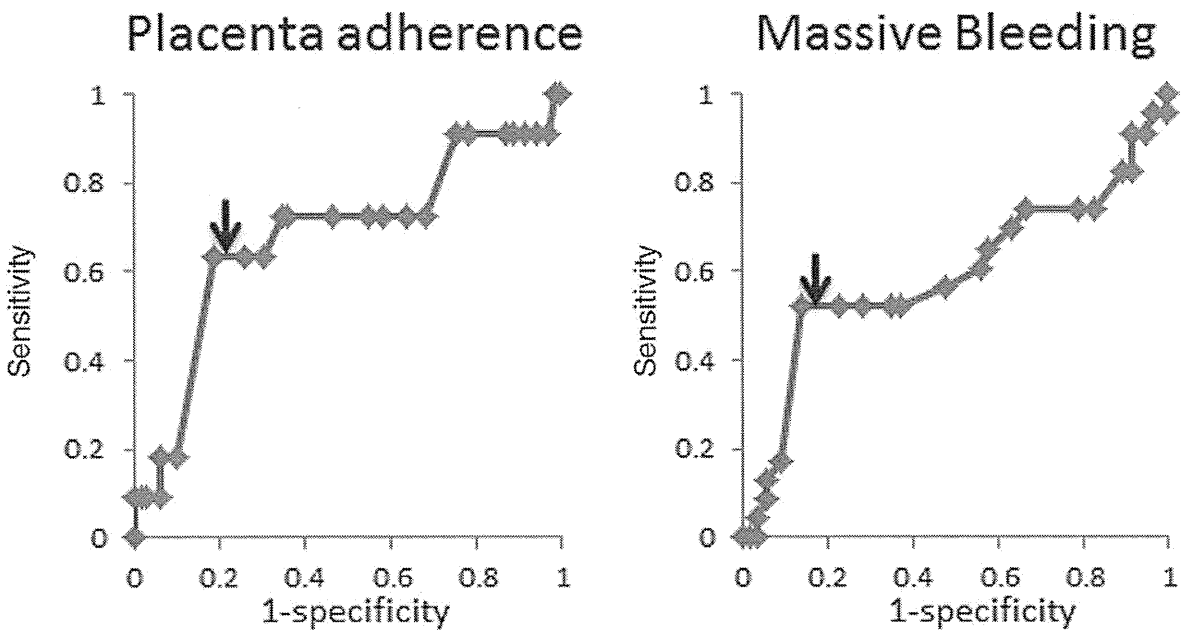

Figure 1 Receiver–operator characteristics curve for cervical length in the prediction of massive bleeding or placental adherence. Arrow denotes a cervical length of 30 mm.

Discussion

Herein we present the retrospective investigation of the relationship between CL and clinical outcomes in cases of placenta previa. Women with placenta previa and a CL of 30 mm or less were more likely to deliver earlier and were at a higher risk for emergent preterm CS than those with longer cervices, consistent with prior reports.[7–9] Moreover, a CL of 30 mm or less was a significant risk factor for both of massive EBL and placental adherence even in multivariate analysis including history of a prior cesarean, anterior placenta, and complete previa, which are conventional risk factors.[10–12] The risk for APH and preterm labor, however, were not significantly higher in the shorter CL group in our series. One possible explanation is that preterm labor may have been reduced by our routine use of tocolytic agents as more patients in the shorter CL group received a tocolytic. It is plausible that the usage of a tocolytic agent could also modify the timing of delivery and other clinical outcomes.

The EBL at CS and the rate of cesarean hysterectomy were significantly higher in the shorter CL group in our study. While the inclusion and reporting criteria and definitions for adherence are not uniform across all studies, our findings are consistent with what has been previously reported.[7,8]

Our series included one case of a cervicoisthmic pregnancy diagnosed at nine weeks of gestation. Following appropriate counseling, the patient opted to continue the pregnancy. There are only two cases describing the conservative management of this type of pregnancy in the literature.[13,14] In these cases, marked cervical shortening was noted, with a residual length of only 17 mm at 14 weeks[15] and at 10 weeks.[14] In the present case, ultrasonography at 28 weeks of pregnancy demonstrated findings consistent with a typical placenta previa with a CL of 18 mm. Despite the short cervix, this pregnancy was not complicated by preterm labor. The placenta was implanted on the posterior uterine wall, and was low-lying, extending to the cervicoisthmic junction. Complete extraction of the placenta was not possible at the time of CS, thus a portion was left *in situ*. Conservative management of the retained placenta was done as previously reported.[16]

We excluded patients with a history of significant uterine activity prior to the initial CL measurement. In addition, in the case of patients presenting with APH, regardless of perceived contractions, uterine activity was assessed with a tocogram. Only two cases of seven

© 2011 The Authors
Journal of Obstetrics and Gynaecology Research © 2011 Japan Society of Obstetrics and Gynecology

patients with placental adherence in the shorter CL had an APH and only one case resulted in preterm delivery at 30 weeks due to a massive APH. Taken together with the findings from the case of cervicoisthmic pregnancy, it is possible that some of the patients with shorter CL at late 2nd or early 3rd trimester in placenta previa implicate not cervical priming but placental insertion to lower part of uterus, which causes APH or placental adherence.[13]

Sonographic findings suggestive of a placenta accreta have been previously reported.[13,14,16] The presence of both a myometrial thickness of 1 mm and less accompanied by large placental lakes carries a PPV of accreta of 72%.[17] Disruption of the placental-uterine wall interface and the presence of vessels crossing this area are the most valuable predictive criteria (89% sensitivity and 98% specificity).[18] The numbers of patients with placental adherence included in these studies, however, are small and there is not uniform agreement regarding which factors are most accurate in the diagnosis of placental adherence.[14,16] The sensitivity and specificity of CL in our series is similar to other reports. The inclusion of other ultrasonographic findings including placental lacuna and the loss of the clear zone did not increase the PPV in our study over what was obtained using CL alone as all cases with these findings were already involved in the shorter CL group. These sonographic markers, however, may still be useful to survey for at the time of CL measurement as they are easy to obtain and may direct further workup. The combination of MRI findings with sonographic markers also might elevate the accuracy of predicting maternal outcomes.[15] In conclusion, we have demonstrated that a shorter CL is associated with an increased risk of emergent preterm CS and increased intrapartum blood loss in the setting of placenta previa. Thus CL should be an additional assessment parameter in the evaluation of a placenta previa.

Acknowledgments

This work was supported in part by a grant-in-aid from the Japan Ministry of Education (20591301).

References

1. Obstetrical hemorrhage. In: Cunningham FG, Leveno KJ, Bloom SL, Hauth JC, Rouse DJ, Spong CY (eds). *Williams Obstetrics*, 23rd edn. New York: McGraw-Hill, 2010; 757–803.
2. Publications Committee, Society for Maternal-Fetal Medicine, Belfort MA. Placental adherence. *Am J Obstet Gynecol* 2010; **203**: 430–439.
3. Oppenheimer L. Society of obstetricians and gynaecologists of Canada: Diagnosis and management of placenta praevia. *J Obstet Gynaecol Can* 2007; **29**: 261–273.
4. Iams JD, Goldenberg RL, Meis PJ *et al.* The length of the cervix and the risk of spontaneous premature delivery: National institute of child health and human development maternal fetal medicine unit network. *N Engl J Med* 1996; **334**: 567–572.
5. Owen J, Yost N, Berghella V *et al.* Mid-trimester endovaginal sonography in women at high risk for spontaneous preterm birth. *JAMA* 2001; **286**: 1340–1348.
6. Hibbard JU, Tart M, Moawad AH. Cervical length at 16–22 weeks' gestation and risk for preterm delivery. *Obstet Gynecol* 2000; **96**: 972–978.
7. Stafford IA, Dashe JS, Shivvers SA, Alexander JM, McIntire DD, Leveno KJ. Ultrasonographic cervical length and risk of hemorrhage in pregnancies with placenta previa. *Obstet Gynecol* 2010; **116**: 595–600.
8. Zaitoun MM, El Behery MM, Abd El Hameed AA, Soliman BS. Does cervical length and the lower placental edge thickness measurement correlates with clinical outcome in cases of complete placenta previa? *Arch Gynecol Obstet.* DOI: 10.1007/s00404-010-1737-1.
9. Ghi T, Contro E, Martina T *et al.* Cervical length and risk of antepartum bleeding in women with complete placenta previa. *Ultrasound Obstet Gynecol* 2009; **33**: 209–212.
10. Robinson BK, Grobman WA. Effectiveness of timing strategies for delivery of individuals with placenta previa and accreta. *Obstet Gynecol* 2010; **116**: 835–842.
11. Sumigama S, Itakura A, Ota T *et al.* Placenta praevia increta/percreta in Japan: A retrospective study of ultrasound findings, management, and clinical course. *J Obstet Gynaecol Res* 2007; **33**: 606–611.
12. Ghourab S. Third-trimester transvaginal ultrasonography in placenta praevia: Does the shape of the lower placental edge predict clinical outcome? *Ultrasound Obstet Gynecol* 2001; **18**: 103–108.
13. Strobelt N, Locatelli A, Ratti M, Ghidini A. Cervico-isthmic pregnancy: A case report, critical reappraisal of the diagnostic criteria, and reassessment of the outcome. *Acta Obstet Gynecol Scand* 2001; **80**: 586–588.
14. Honda T, Hasegawa M, Nakahori T *et al.* Perinatal management of cervicoisthmic pregnancy. *J Obstet Gynaecol Res* 2005; **31**: 332–336.
15. Lam G, Kuller J. Use of magnetic resonance imaging and ultrasound in the antenatal diagnosis of placenta accreta. McMahon M. *J Soc Gynecol Investig* 2002; **9**: 37–40.
16. Sentilhes L, Kayem G, Ambroselli C *et al.* Fertility and pregnancy outcomes following conservative treatment for placenta accreta. *Hum Reprod* 2010; **25**: 2803–2810.
17. Twickler DM, Lucas MJ, Balis AB *et al.* Color flow mapping for myometrial invasion in women with a prior caesarean delivery. *J Matern Fetal Med* 2000; **9**: 330–335.
18. Wong HS, Cheung YK, Zuccollo J, Tait J, Pringle KC. Evaluation of sonographic diagnostic criteria for placenta accreta. *J Clin Ultrasound* 2008; **9**: 551–559.

© 2011 The Authors
Journal of Obstetrics and Gynaecology Research © 2011 Japan Society of Obstetrics and Gynecology

Clin Pediatr Endocrinol 2011; 20(4), 95-98
Copyright© 2011 by The Japanese Society for Pediatric Endocrinology

Case Report

Fabry Disease Superimposed on Overt Autoimmune Hypothyroidism

Noriyuki Katsumata[1, 2], Akira Ishiguro[2], and Hiroshi Watanabe[2]

[1]*Department of Molecular Endocrinology, National Research Institute for Child Health and Development, Tokyo, Japan*

[2]*Department of Pediatrics, Mizonokuchi Hospital, Teikyo University School of Medicine, Kawasaki, Japan*

Abstract. Fabry disease (FD) is an X-linked recessive disorder caused by lysosomal α-galactosidase A deficiency. FD is characterized by the systemic accumulation of globotriaosylceramide with involvement of the heart, kidney, brain and gastrointestinal system. Recently, nonautoimmune thyroid dysfunction was recognized as an additional clinical feature of FD. In the present study, we describe a patient suffering from FD superimposed on overt autoimmune hypothyroidism. The patient was an 11-yr-old boy who presented with goiter and stunted growth, and was diagnosed with primary hypothyroidism due to autoimmune thyroiditis. During levothyroxine replacement therapy, the patient complained of burning pain in his feet and was diagnosed as suffering from FD based on low blood α-galactosidase A activity. In conclusion, we have described the first FD patient preceded by overt autoimmune hypothyroidism.

Key words: Fabry disease, α-galactosidase A, globotriaosylceramide, autoimmune thyroiditis, hypothyroidism

Introduction

Fabry disease (FD) is an X-linked recessive disorder caused by lysosomal α-galactosidase A deficiency and is characterized by the systemic accumulation of globotriaosylceramide (1). FD is recognized as a multiorgan disease with involvement of the heart, kidney, brain and gastrointestinal system (2). Recently, endocrine dysfunctions including subclinical hypothyroidism add to the clinical picture of FD (3–6).

In the present study, we report an FD patient who first presented with overt autoimmune hypothyroidism.

Received: June 17, 2011
Accepted: August 29, 2011
Correspondence: Dr. Noriyuki Katsumata, Department of Molecular Endocrinology, National Research Institute for Child Health and Development, 2-10-1 Okura, Setagaya-ku, Tokyo 157-8535, Japan
E-mail: nkatsumata@nch.go.jp

Case Report

The patient is a boy born to a healthy Japanese father and a white American mother. The mother was diagnosed with autoimmune hypothyroidism at 30 yr of age and was started on thyroid hormone replacement therapy. No detailed maternal family history was available. The patient has one sibling, a healthy younger brother. The patient was a product of an uncomplicated 42-wk gestation and delivery. His birth weight was 3,230 g and his birth length